Goethe University Frankfurt am Main
Department of Molecular and Cellular Neurobiology

Thesis submitted for the degree

Bachelor of Science

Neurovascular Interface in Aging Zebrafish

by

Daria Bogatova
Matricule Nr. **6980735**

Supervisor: **Prof. Dr. Amparo Acker-Palmer**
Appraiser: **Prof. Dr. Amparo Acker-Palmer**
Second appraiser: **Dr. Jasmin Hefendehl**

May 2021

To Dima!

No matter how much I say I love you, I always love you more than that. You make me better and happier every day. You are my dream that came true. Thank you for being you, my love!

Acknowledgments

I would like to express my deepest appreciation to my advisor Dr. Bettina Kirchmaier for the great amount of assistance, patience and an unwavering support throughout my University journey. I am also grateful to future Drs Helene Juul Belling and Lukas Euler who not only proved to be spectacular tutors, but also became my dearest friends. I also wish to thank Prof. Dr. Acker-Palmer for her wise guidance and sympathetic ear. Finally, I would like to acknowledge Dmytro Bogatov and Oleksandr Narykov for the insightful suggestions and valuable advice.

This work would not have been possible without all these people, and I am beyond grateful for the opportunity to know every each of them.

Acronyms

Aβ	Amyloid Beta
AD	Alzheimer's Disease
ALCAM	Activated Leukocyte Cell Adhesion Molecule
AQP4	Aquaporin 4
BBB	Blood-Brain Barrier
BDNF	Brain-Derived Neurotrophic Factor
CART4	Cocaine- and Amphetamine-Regulated Transcript 4
CLDN19	Claudin 19
CLDN5	Claudin 5
CNR1	Cannabinoid Receptor 1
CNS	Central Nervous System
CNTF	Ciliary Neurotrophic Factor
CSR	Chronic Sleep Restriction
CX47	Connexin 47
EC	Endothelial Cell
GDNF	Glial Cell-Line Derived Neurotrophic Factor
HE	Hematoxylin-Eosin
HM	Hybridization Mix
IL-1β	Interleukin-1β
IL-6	Interleukin-6
MAG	Myelin-Associated Glycoprotein

MANF	Mesencephalic Astrocyte-Derived Neurotrophic Factor
MHC1	Major Histocompatibility Complex 1
MMP3	Metallopeptidase 3
NADL1.2	Neural Cell Adhesion Molecule L1
NDS	Normal Donkey Serum
NEUROD	Neurogenic Differentiation
NFASCA	Neurofascin
NGF	Nerve Growth Factor
NR3C1 α	Glucocorticoid Receptor α
NR3C1 β	Glucocorticoid Receptor β
NR3C2	Mineralocorticoid Receptor
NVU	Neurovascular Unit
OPC	Oligodendrocyte Precursor Cell
PAS	Periodic Acid-Schiff
PBS	Phosphate Buffer Saline
PCNA	Proliferating Cell Nuclear Antigen
PD	Parkinson's Disease
PFA	Paraformaldehyde
RT	Room Temperature
SASP	Senescence-Associated Secretory Phenotype
SSC	Saline-Sodium Citrate
SVZ	Subventricular Zone
TIMD4	T-Cell Immunoglobulin and Mucin Domain Containing 4
TJ	Tight Junction
TNF-α	Tumor Necrosis Factor-α
VSMC	Vascular Smooth Muscle Cell
WHO	World Health Organization

Contents

Acknowledgments iii

Acronyms iii

Contents vi

List of Figures viii

List of Tables ix

1 Summary 1

2 Introduction 2

2.1 Neurovascular Unit and Aging . . . 2

2.2 Blood-Brain Barrier . . . 8

2.2.1 Role of Claudin in Blood-Brain Barrier . . . 9

2.3 Blood-Brain Barrier During Aging . . . 10

2.4 Zebrafish as Gerontology Model . . . 12

2.5 Integrative Hallmarks of Aging . . . 13

3 Our Aims 16

3.1 Methodological Aim . . . 16

3.2 Scientific Aim . . . 16

4 Materials and Methods 17

4.1 Materials . . . 17

4.2 Brain Sectioning . . . 18

4.3 Staining . . . 19

4.4 Imaging . . . 20
4.5 Hybridization . . . 20
4.5.1 Rehydration . . . 20
4.5.2 Permeabilization . . . 21
4.5.3 Postfixation . . . 21
4.5.4 Prehybridization . . . 21
4.5.5 Hybridization . . . 21
4.5.6 Preparation for day 2 . . . 21
4.5.7 Posthybridization washes (performed at 70 °C) . . . 22
4.5.8 Preincubation washes (performed at room temperature (RT)) . . . 22
4.5.9 Blocking and antibody incubation . . . 22
4.5.10 Equilibration steps . . . 23
4.5.11 Staining . . . 23

5 Results **24**

6 Discussion **33**

6.1 Does aging in Zebrafish occur gradually like in mammals? . . . 33
6.2 What happens to BBB during aging? . . . 35
6.3 Does aging affect vessel density? . . . 36

7 Further Study **38**

A *in-situ* Hybridization **40**

B Heart Staining Protocol **41**

B.1 Tris-EDTA Buffer Antigen Retrieval Protocol (pH 9) . . . 42
B.2 Citrate Buffer Antigen Retrieval Protocol (pH 6) . . . 42

Bibliography **45**

List of Figures

2.1 Neurovascular Unit Overview 3

2.2 The impact of aging on the neurovascular unit components 4

2.3 Dysfunction of cells in AD 6

2.4 BBB disruption in PD 7

2.5 Structure of claudin-5 9

2.6 Multifactorial Modulation of Blood-Brain Barrier Integrity 11

2.7 Hallmarks of aging in Zebrafish 13

4.1 Brain Sectioning and Staining 18

5.1 Telencephalon of 11 m.o. Zebrafish 25

5.2 Telencephalon of 24 m.o. Zebrafish 26

5.3 CLDN5 and Vessel Density 27

5.4 CLDN5 and Vessel Density Imaris Images 28

5.5 CLDN5 Coverage 29

5.6 tg(kdrl:eGFP)^{s843} Coverage Imaris Images 30

5.7 CLDN5 Coverage Imaris Images 31

5.8 CLDN5 Coverage Merged Imaris Images 32

A.1 *in situ* Hybridization Midbrain 40

B.1 Heart Staining 41

List of Tables

4.1 Fish Strain 17
4.2 Antibodies 17
4.3 Chemicals 18
4.4 Equipment and Software 19

B.1 Antibodies for Tris-EDTA Buffer Antigen Retrieval Protocol 43
B.2 Antibodies for Citrate Buffer Antigen Retrieval Protocol 44

Chapter 1

Summary

Apprehending molecular mechanisms of aging appears to be a major challenge for modern science due to the versatility of the senescence process and the paucity of animal models. The age of the world's population, however, keeps increasing, therefore, the main goal of our work was to investigate the process of deterioration within Zebrafish to explore further perspectives for this model organism. For this purpose we decided to start with Telencephalon, the region that is responsible for the majority of cognitive functions.

During our project we established a new protocol for the brain sections staining that fits the purposes of the study. Most importantly, we answered the questions whether Zebrafish deteriorates gradually and whether aging affects vessel density and blood-brain barrier quality. Our data revealed that even at 24 months of age the levels of Claudin5 remain in normal range, thus, ensuring normal permeability of BBB. The number of vessels, conversely, turned out to be greatly decreased.

This study is the first one to be conducted on a Zebrafish brain vascular system and we can proudly acknowledge that the results we acquired not only correlate well with the most recent literature, but also bring a novel outlook on this model organism for aging investigation.

Chapter 2

Introduction

According to the World Health Organization (WHO) the proportion of the world's population over 60 years will nearly double from 12 % to 22 % between the years 2015 and 2050. Moreover, the pace of population aging is increasing nowadays (Steverson, 2018). This makes aging, and age-related senescence of Central Nervous System (CNS) in particular, one of the most important areas of modern research.

2.1 Neurovascular Unit and Aging

A relatively new concept in neuroscience, NVU, is another important thing to consider while discussing aging. Neurovascular unit is defined as a functional unit with multiple components in CNS, including vascular cells such as pericytes, Vascular Smooth Muscle Cells (VSMCs), endothelial cells; glial cells such as astrocytes, microglia, oligodendrocytes, and lastly neurons (Banks et al., 2018). Its dysfunction can be differentiated into two categories: normal aging or cell senescence, and pathological NVU dysfunction due to cerebral ischemic stroke or neurodegenerative diseases. With aging, all components of the NVU undergo significant changes, including neurons, glial cells, vascular cells as well as the basal lamina matrix within the brain vasculature (Figure 2.2) (Cai et al., 2017).

Neurons, due to their high metabolic rate, appear to be the cell type that is the most susceptible to aging associated cell injuries. Their capacity for ROS clearance is signifi-

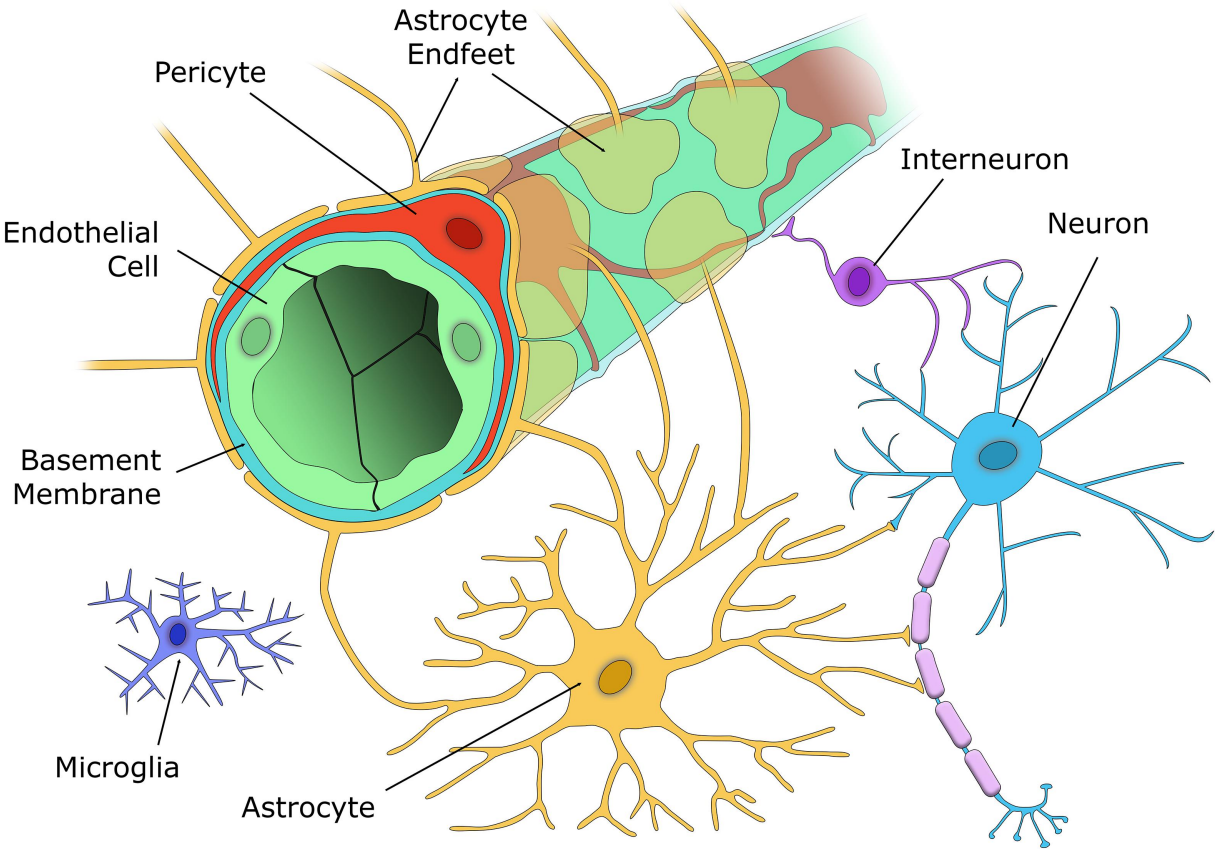

Figure 2.1: Neurovascular Unit Overview. The capillary wall of Neurovascular Unit (NVU) contains a single layer of ECs (green) connected by tight junctions. Along with pericytes (red), that are embedded within the capillary basement membrane (turquoise), and astrocyte end-feet (yellow), they form the Blood-Brain Barrier (BBB). Excitatory neurons (light blue) synapse with vasoactive interneurons (purple) and astrocytes (yellow). Microglia (blue) are located in the brain parenchyma and respond to any aversive stimuli protecting the brain from damages. By Brown et al. (2019).

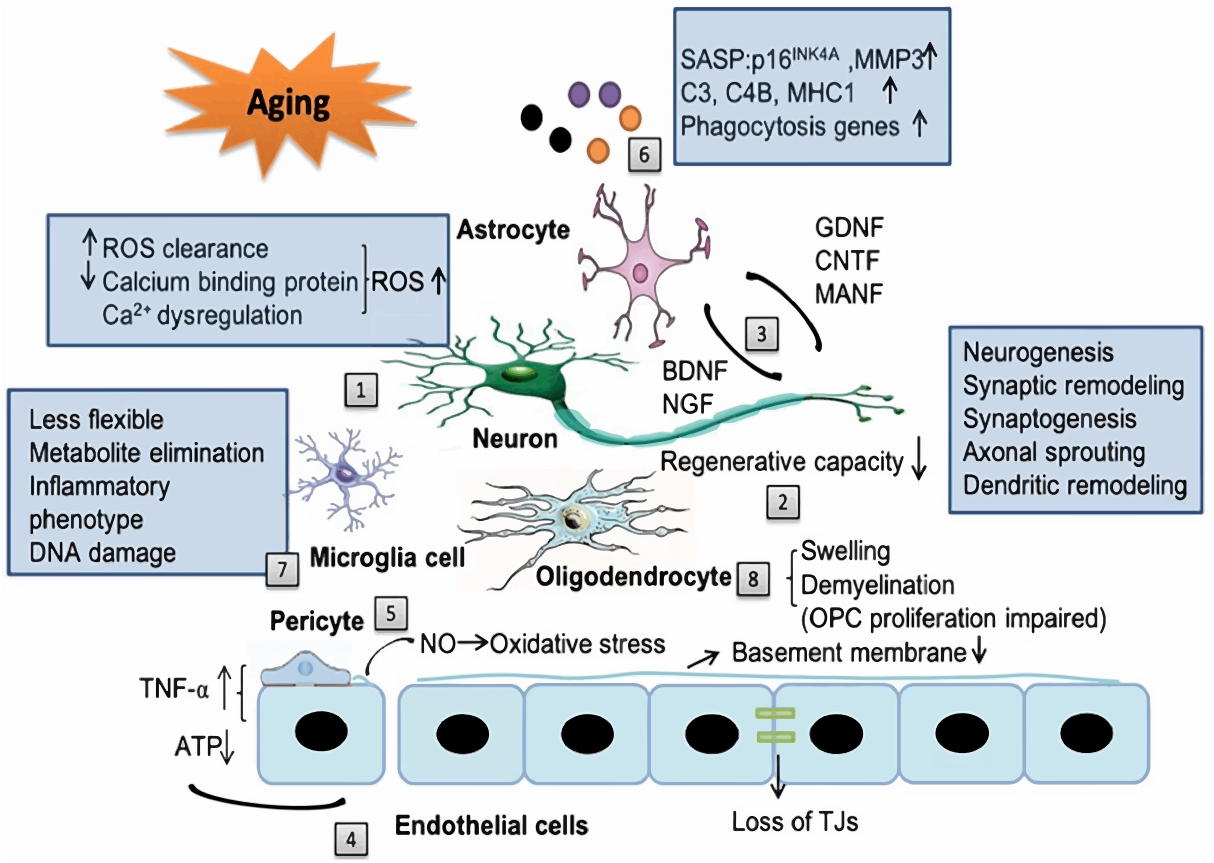

Figure 2.2: The impact of aging on the neurovascular unit components. **1** Reduced ROS clearance capacity, decreased expression of calcium binding proteins, Ca^{2+} dysregulation and increased ROS production promote the aggravation of neuronal injury. **2** Throughout the aging regenerative capacities also decline. This includes neurogenesis, synaptic remodeling, synaptogenesis, axonal sprouting and dendritic remodeling. **3** Neurotrophic factors such as BDNF, NGF, GDNF, CNTF and MANF are reduced which contributes to cognitive decline. **4** Endothelial cells start secreting some noxious factors, such as TNF-α and consume increased amount of ATP. Moreover, the thickness of basement becomes decreased and TJ undergo disruption. **5** With age pericytes generate more nitric oxide (NO), thus further increase the oxidative stress in the NVU. **6** Astrocytes start expressing Senescence-Associated Secretory Phenotype (SASP), such as $p16^{\text{INK4A}}$, MMP3, complement system genes (C3 and C4B) and major Major Histocompatibility Complex 1 (MHC1). They also start upregulating phagocytosis genes, which enhance neuroinflammation following cognitive decline. **7** Microglia develop neuroinflammatory phenotype, become less flexible and decreases their capacity to eliminate metabolites, therefore accumulate more DNA damages. **8** Lastly, oligodendrocytes acquire swelling morphology and persuade broad and irreversible demyelination which impairs the ability of OPCs to proliferate. From Li et al. (2019).

cantly reduced with aging, leading to an increased sensitivity to oxidative stress (Mattson & Magnus, 2006). Dysregulation of calcium and decreased expression of calcium binding proteins contribute to further ROS production, thus exacerbating NVU injury in the aging brain. Moreover, neuronal regenerative capacities also decline. This includes neurogenesis, synaptic remodeling, synaptogenesis, axonal sprouting and dendritic remodeling (Skaper et al., 2017). Furthermore, certain neurotrophic factors that ensure proper neuron-glial interaction appear to be reduced with age. This includes neuron-produced factors, such as Brain-Derived Neurotrophic Factor (BDNF) and Nerve Growth Factor (NGF), that are crucial for the normal NVU function (Budni et al., 2015). It also involves glia-produced factors, such as Glial Cell-Line Derived Neurotrophic Factor (GDNF), Ciliary Neurotrophic Factor (CNTF) and Mesencephalic Astrocyte-Derived Neurotrophic Factor (MANF) that control synaptic and neuronal growth, pruning, myelination and neuronal cell survival (Pöyhönen et al., 2019). All these events contribute to cognitive decline and neuronal functions impairment.

Vascular part of NVU also undergoes aging and the main component here is Endothelial Cells (ECs). Senile ECs start secreting some noxious factors, such as Tumor Necrosis Factor-α (TNF-α) and consume increased amount of ATP (Banks et al., 2018). This makes them vulnerable to oxidative stress and it increases the permeability of BBB. Moreover, decreased thickness of basement membrane, disruption of Tight Junctions (TJs) and reduction of trophic factors from brain pericytes contribute to age-associated injury of NVU.

Lastly, it is important to descry aging in glial cells. Astrocytes constitute the main part of glia and in the aging brain they start expressing SASP proteins, which disrupt the functional neuron-glial interaction by turning them into proinflammatory phenotypes. $p16^{\mathrm{INK4A}}$ and Metallopeptidase 3 (MMP3) enhance age-related neuroinflammation and exacerbates the functional decline of the aging brain (Baker & Petersen, 2018).

Microglia is considered the main executor of inflammation after acute and chronic brain injuries (Kluge et al., 2019). With aging they develop neuroinflammatory pheno-

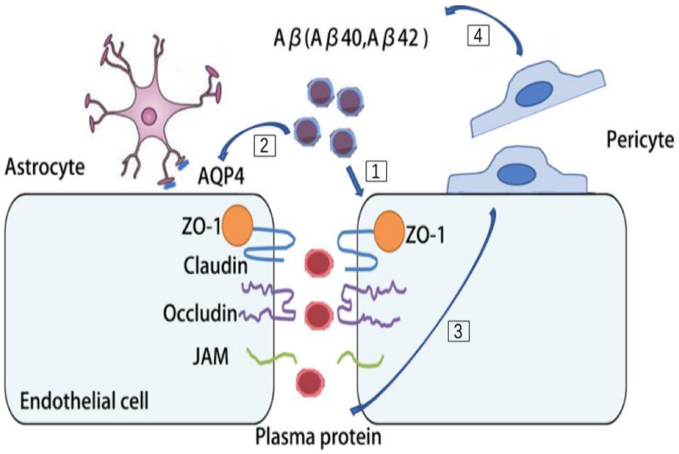

Figure 2.3: Disfunction of cells in AD. **1** Aβ42 disrupt the organization of TJs and adherent junction in endothelial cells. **2** Aβ42 burden redistribute AQP4 on astrocytes and cause retraction and swelling of astrocytic end-feet. **3** Pericytes detach from microvessels and cause leakage of plasma protein. **4** Pericytes deficiency causes accelerated brain Aβ42 deposition. From Li et al. (2019).

type, become more rigid and lose their flexibility and the ability to eliminate endogenous metabolites, thus accumulating more mutations and DNA damages (Perry & Holmes, 2014).

Oligodendrocytes is another cell type that develops swelling morphology through degenerated myelin sheaths in the cytoplasm. Demyelination results in exposure of unwrapped axons, which should stimulate the proliferation of OPCs and remyelination. In the aged brain, however, the velocity of remyelination is significantly decreased which causes progressive neurological deteriorations in individuals with neurodegenerative disorders (Peters, 2009).

Summarizing all aforementioned, it is clear that aging affects all the components of the NVU. It might as well impact the cell-cell interaction within the NVU and consequently lead to NVU dysfunction and compromised BBB.

Alzheimer's Disease (AD) is one of the most common neurodegenerative pathologies associated with age where NVU plays one of the main roles. It accounts for up to 80 % of all dementia cases (Crous-Bou et al., 2017) and is characterized by a progressive decline in two or more cognitive domains such as memory, speech, executive and visuospatial function,

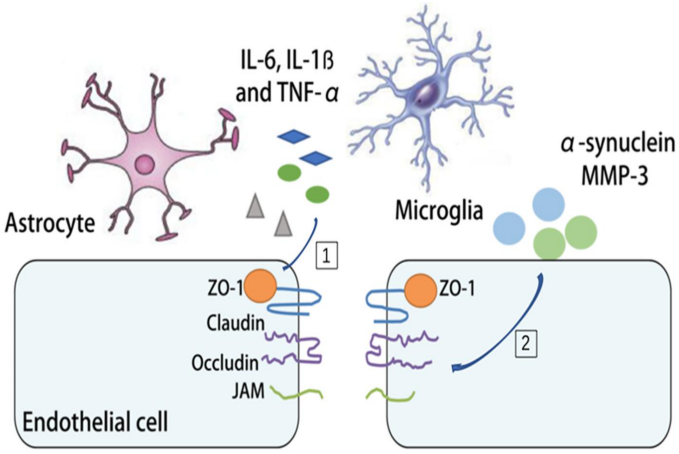

Figure 2.4: BBB disruption in PD. **1** The rearrangement of TJs during PD causes the release of Interleukin-6 (IL-6), Interleukin-1β (IL-1β) and TNF-α by microglia and astrocytes. **2** BBB permeability and neuroinflammation in PD are increased due to the deposition of α-synuclein and MMP3. From Li et al. (2019).

personality, and behavior (Weller & Budson, 2018). In case of AD the impairment of NVU might be the cause as BBB breakdown seems to be an early biomarker of human cognitive dysfunction (Nation et al., 2019). It has been found in the postmortem brain of AD patients that TJ proteins such as occludin, claudin-5, and ZO-1 were significantly reduced in capillaries suggesting that it may cause increased fibrinogen leakages in the brain parenchyma. Therefore, it is likely that Aβ42 disrupts the organization of TJs and adherent junction between endothelial cells, thus distorting their barrier abilities (Figure 2.3). Moreover, high degree of Aβ burden causes redistribution and sometimes even loss of Aquaporin 4 (AQP4) on end-foot membranes of astrocytes causing their retraction and swelling (Zeppenfeld et al., 2017). Pericytes coverage of vessels is also significantly reduced in brains with AD and it may aggravate hypoperfusion and Aβ clearance impairment (Dalkara et al., 2011). Thus, it is logical to conclude that AD is clearly associated with NVU dysfunction.

The next common neurodegenerative issue is Parkinson's Disease (PD). It is a progressive long-term disorder characterized by both motor and non-motor features. The motor symptoms of PD are linked to the loss of striatal dopaminergic neurons; non-motor symp-

toms, on the other hand, are caused by neuronal loss in nondopaminergic areas. Some researchers suggest that the pathophysiological changes associated with PD might appear before the noticeable onset of motor features. They may include such manifestations as sleep disorders, depression and cognitive changes (Schrag et al., 2015).

There are two aspects to the relationship between NVU and PD. Physiological aging is the first one and it manifests itself as an increased oxidative stress, disturbed mitophagy, reduced energy support and impaired mitochondria repair. It leads to dopaminergic neuronal cell injury and eventually cell loss. The second one is the pathological change of the PD brain. α-synuclein deposition and increased MMP3, for instance, can alter BBB permeability and neuroinflammation. Furthermore, there is a clear evidence of BBB disruption in PD patients (Lee & Pienaar, 2014).

2.2 Blood-Brain Barrier

Blood-Brain Barrier (BBB) is a part of the NVU and is a highly selective semipermeable border consisting of Endothelial Cells (ECs) that limits the passage of solutes in the circulating blood into the extracellular fluid of CNS (Daneman & Prat, 2015). It is formed by capillary wall endothelial cells, astrocyte end-feet, and pericytes that are embedded in the capillary basement membrane (Figure 2.1). The main function of BBB is to maintain a homeostasis of the brain by preventing the passage of pathogens as well as protecting the brain from hormones and neurotransmitters in the rest of the body. It also does not allow large or hydrophilic molecules to pass into the cerebrospinal fluid, while permitting the diffusion of small non-polar molecules and hydrophobic molecules such as O_2 and CO_2 (Shatzmiller et al., 2019).

The stability of BBB is accomplished by ECs that are rigidly sealed by tight and adherent junctions, which restrict the paracellular transport of blood-borne molecules. The ECs are surrounded by mural cells such as pericytes or smooth muscle cells that are embedded in the basal lamina. Furthermore, astrocytic end-feet ensheathe the vessels and

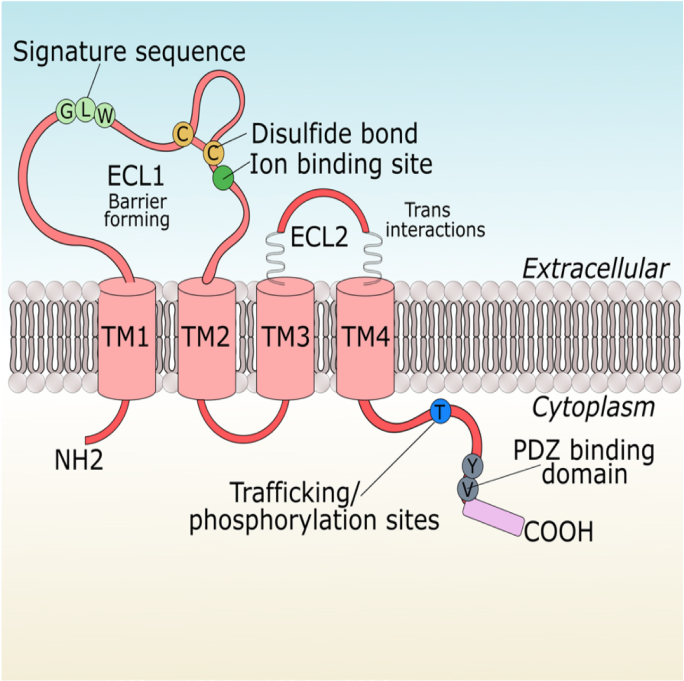

Figure 2.5: Structure of claudin-5. 4 transmembrane domains (TM), a short NH_2 terminus, two extracellular loops, a short intracellular loop and a long COOH terminus create Claudin5 protein. First extracellular loop contains a disulphide bond, ion binding and a highly conserved signature motif. The long COOH terminus contains the PDZ binding motif for interactions with scaffolding proteins. It also includes residues from trafficking and phosphorylation. Adapted from Krause et al. (2008) by Greene et al. (2019).

mediate neurovascular communication. BBB permeability is regulated by the interactions between these different cell types at the neurovascular unit.

2.2.1 Role of Claudin in Blood-Brain Barrier

Tight Junctions (TJs) are the type of cell-cell contact in the lateral membrane between polarized cells, such as those existing in endothelia and epithelia. Their grade of tightness varies significantly in different organs: in a bladder, for instance, the paracellular cleft is almost closed for solutes. Some segments of renal tubules, on the other hand, have paracellular pores formed for specific cations (andanions). The strands of a TJ consist of

various transmembrane proteins, such as occludin (Furuse et al., 1993), tricellulin (Ikenouchi et al., 2005) and claudins (Morita et al., 1999).

Claudins are tetraspan transmembrane proteins that create the structural core of of tight junctions (Furuse, 2010). They are expressed in a tissue specific combination resulting in tissue specific barrier characteristics (Krause et al., 2008). Lack or impairment of claudins is associated with diseases and dysfunction of many organs and tissues such as the inner ear (Wilcox et al., 2001; Florian et al., 2003), epidermis (Furuse et al., 2002; Tebbe et al., 2002), brain capillaries (Nitta et al., 2003; Wolburg et al., 2003), gastrointestinal tract (Resnick et al., 2005; Amasheh et al., 2009) and kidneys (Konrad et al., 2006; Günzel et al., 2009). In mammals, at least 27 members of claudin family are currently described (Mineta et al., 2011). According to the degree of sequence similarity they were differentiated into two groups: classic claudins (1–10, 14, 15, 17, 19) and non-classic ones (11–13, 16, 18, 20–24).

In this work we focused particularly on Claudin-5 as it is a major cell adhesion molecule of TJ of the BBB and according to Ohtsuki et al. (2007) its expression is more than 100 times higher compared to other claudins. Interestingly, Nitta et al. (2003) had discovered that BBB of Claudin-5-deficient mice was preamble to molecules < 800 Da which makes this protein promising to investigate possible ways of delivering drugs through BBB (Brunner et al., 2020). Our exact area of interest, however, is a development in Claudin-5 expression throughout the aging process as its deterioration leads to neurodegenerative disorders such as Alzheimer's Disease, neuroinflammatory disorders like multiple sclerosis and psychiatric disorders such as depression and schizophrenia (Greene et al., 2019).

2.3 Blood-Brain Barrier During Aging

Most of the recent studies describe aging as the time-dependent accumulation of cellular damage. The contributions to cellular damage are interrelated and include oxidative stress, epigenetic changes, genomic instability, telomere attrition, dysregulation of cell

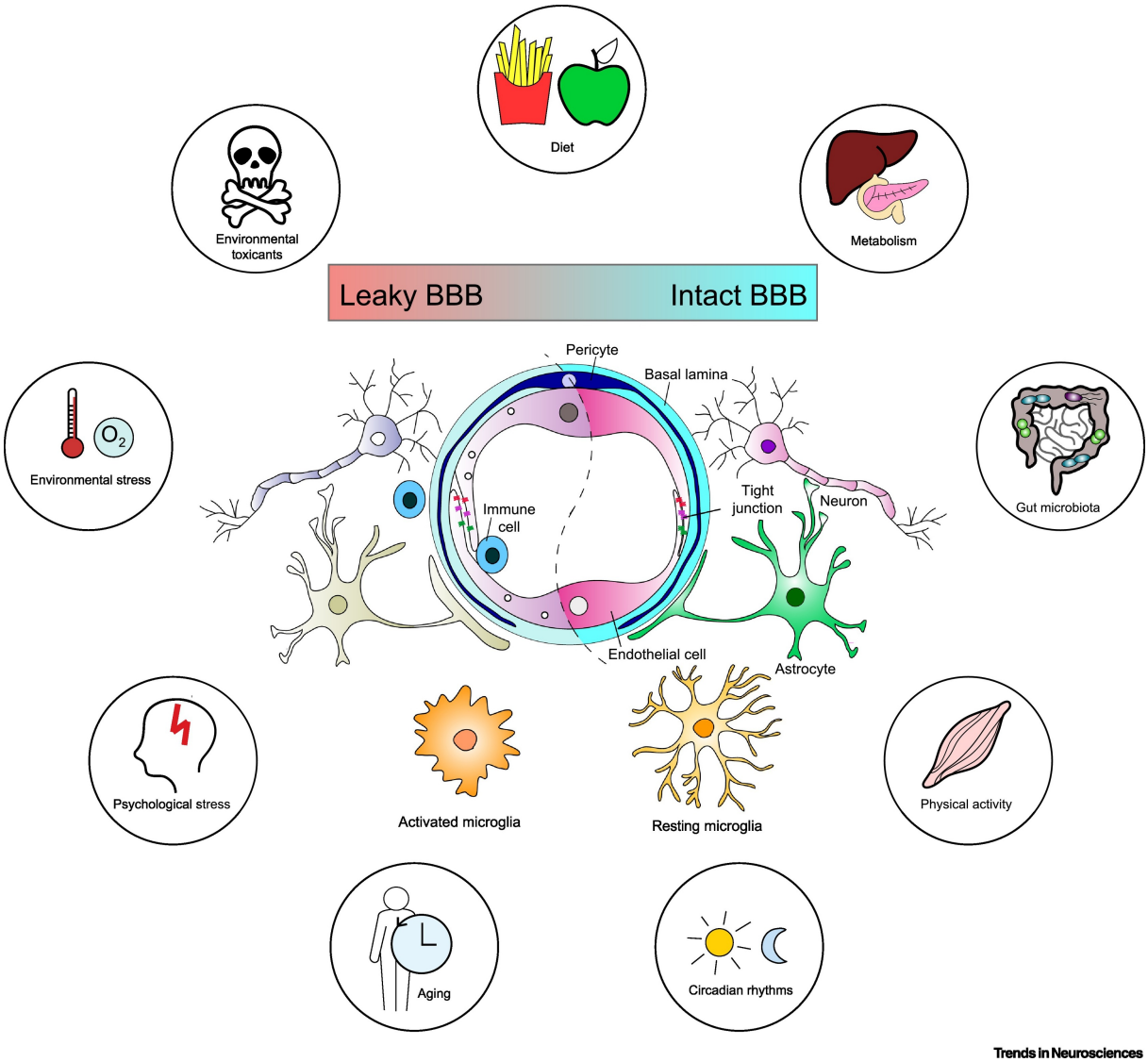

Figure 2.6: Multifactorial Modulation of Blood-Brain Barrier Integrity. A scheme representing intact and leaky BBB along with the factors that might contribute to BBB disruption. Certain lifestyle habits, exposure to stressors and aging may favor BBB leakiness, through opening of tight junctions, increased transcytosis, disrupted neurovascular communication, and neuroinflammation. By Segarra et al. (2021).

signaling and inflammatory responses, and senescence (Banks et al., 2021). Some of the recent works have observed an increased number of brain endothelial cells associated with age, that exhibit high levels of senescence-related gene expression (Kiss et al., 2020). One senescence factor that regulates vBBB is called sirtuin-1; its loss is commonly associated with vBBB dysfunction (Stamatovic et al., 2019). The tightness of the BBB and the crosstalk between its cellular components are highly dynamic and modulated by aforementioned factors and described in Figure 2.6. Alterations in BBB permeability can occur due to physiological conditions as well as due to inflammation processes or disruption in neurovascular communication (Segarra et al., 2021).

In this work we focused on the aging aspects of BBB disruption, since there are studies revealing that BBB permeability in the human hippocampus increases throughout aging, suggesting its contribution to dementia (Montagne et al., 2015). Moreover, it appears to be a biomarker of neurodegenerative disorders such as Alzheimer's Disease and Parkinson's Disease (Nation et al., 2019).

2.4 Zebrafish as Gerontology Model

Due to their convenience Zebrafish (*Danio rerio*) generated substantial interest as a model organism in recent years. Their embryos are transparent which allows proper investigation of the internal structures such as vessels, nerves and muscles, furthermore, the number of offsprings for this kind of fish is extremely high. Most importantly, Zebrafish have certain similarities with the human organism such as the heart rate around 100 bpm, for instance. Moreover, their organs exhibit the main features of the ones in humans. The ability of Zebrafish to regenerate the heart also gives an opportunity to discover possible therapies for cardiac injury (Asnani & Peterson, 2014). They develop relatively fast and the lifespan of these species is short (around 40 months), but like mammals they appear to age gradually which makes them a nearly perfect model organism to interrogate the aging process. Such characteristics resulted in a successful detailed characterization of the Zebrafish genome,

therefore multiple mutant and transgenic phenotypes along with molecular genetics techniques had been developed allowing the exploration of the intrinsic mechanisms underlying normal physiological and pathological events in this organism (Kishi et al., 2009).

2.5 Integrative Hallmarks of Aging

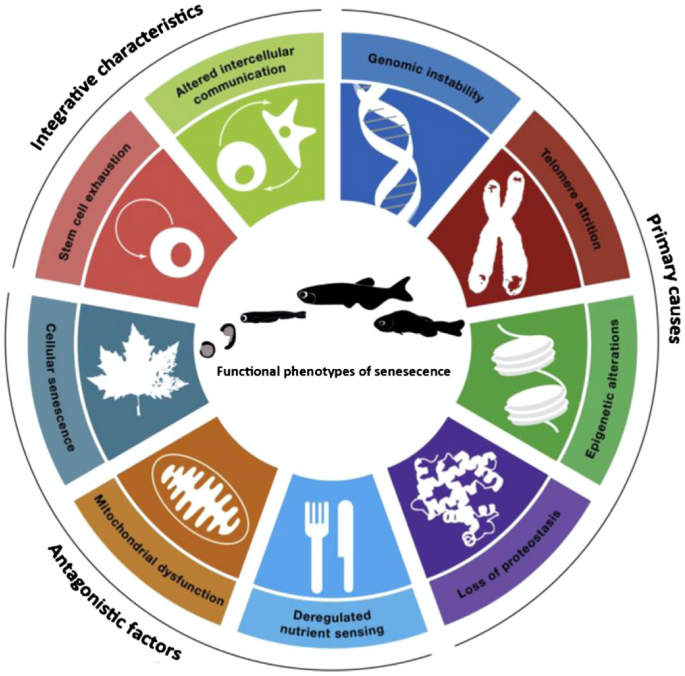

Figure 2.7: Hallmarks of aging in Zebrafish. Nine hallmarks of aging modified for Zebrafish as a gerontology model differentiated into three causes of aging: primary, antagonistic factors and integrative characteristics. Adapted from López-Otín et al. (2013) by Van houcke et al. (2015).

Aging process is not trivial to describe due to the large number of players involved. In Figure 2.7, nevertheless, López-Otín et al. (2013) represented senescence with nine main parameters that are linked to the aging process and Van houcke et al. (2015) modified this figure for Zebrafish model and differentiated these nine parameters into three main causes of aging, and integrative characteristics are the most relevant to our project. The first hallmark in this category is a stem cell exhaustion. It is known that with age proliferation and differentiation of stem and progenitor cells become impaired. In mammals stem cell

potential in a brain is extremely limited and restricted to only Subventricular Zone (SVZ) in hippocampus and the olfactory bulb. Zebrafish, on the other hand, have multiple regions of consistent neuron renewal, and radial glia stem cell potentiation in animal's telencephalon is a main structure for neurogenesis (Ito et al., 2010). The natural stem cell potential past young adulthood, however, was overlooked until recently. It has been discovered that neurogenesis in Zebrafish telencephalon is indeed seriously declining with age (Edelmann et al., 2013). Furthermore, oligodendrogenesis within the telencephalic parenchyma also appears to be impaired, as in the study of Edelmann et al. (2013) the number of dividing oligodendrocytes was significantly reduced in 15-month-old fish, as compared to 5-month-old fish. Moreover, by age-dependent stem cell exhaustion the capacity to regenerate a massive loss in neuronal cells (injury- or pathology-induced) also declines.

The next hallmark is alterations in intercellular communication. Some studies reported that pro-inflammatory cytokines that are mostly secreted by senescent cells, are increasing along with the tissue damage accumulation. Other papers claim an increasing number of microglia and/or macrophages, which appear to become less functional with age (Streit et al., 2004). The same study concluded that even more inflammatory cells are invading after brain injury in order to restore homeostasis. In 18-month-old Zebrafish fewer microglia and macrophages in the optic nerve at four days post myelin damage were observed, as compared to young ones (Münzel et al., 2014).

Finally, it is important to also mention functional phenotypes of senescence. For our project one of the crucial things to keep in mind was the theory that, just like mammals, Zebrafish appear to age gradually. There are not many studies done in this area, but in one of them a slow progression of retinal atrophy with age was visualized in 20- to 58-month-old Zebrafish (Kishi et al., 2009). Our experiments and statistical data also seem to support this statement.

Lastly, it has been established that inhibitory avoidance performance is impaired in 24-month-old fish, when compared to young ones. With the age it is noticeable that

the telencephalic expression of genes related to plasticity and learning (*bdnf*, *pcna*, and *neurod*), as well as the neuroendocrine system (*cart4*, *htr1ab*, and *crf-bp*), is being reduced (Manuel et al., 2015). Thus, fish over 24 months demonstrate diminished speed of learning.

Chapter 3

Our Aims

In this project we had two categories of aims: a methodological and a scientific one.

3.1 Methodological Aim

The first goal was to establish staining and sectioning protocols that will work for visualizing vessel density and CLDN5 distribution.

During our work we developed methods for staining the sections of an aging brain as well as a protocol for *in-situ* hybridization. We have also performed imaging on Zebrafish brains and hearts. Finally, we completed a statistical analysis about vessel and Claudin5 coverage.

3.2 Scientific Aim

Our goal here was to investigate the aging process within Zebrafish model. For this purpose we raised several questions that we are going to answer in the Discussion part:

1. Does aging in Zebrafish occur gradually like in mammals?
2. What happens to BBB during aging?
3. Does aging affect vessel density?

Chapter 4

Materials and Methods

4.1 Materials

For the project two aging groups of Zebrafish were dissected.

Table 4.1: Fish Strain

Family Nr.	Age Born	Reporter Line	Description	Literature
602	11 months March 12th 2020	tg(kdrl:eGFP)^{s843}	GFP Expression in vascular system	(Jin et al., 2005)
446	24 months February 7th 2019	tg(kdrl:eGFP)^{s843}/ tg(gata)1 : (dsRed)^{sd2}	GFP Expression in vascular system DsRed Expression in blood cells	(Jin et al., 2005) (Traver et al., 2003)

Table 4.2: Antibodies

	Name	Host	Clone	Company	Dilution	Staining
1 AB	Claudin5	Mouse	4C3C2	LifeTech/ Invitrogen	1 : 700	TJs
	GFAP	Rabbit	polyclonal	DAKO	1 : 700	Glia
			Antigen			
2AB	Alexa_647	Donkey	anti-mouse IgG	MolProbes	1 : 800	
	Alexa_555	Donkey	anti-rabbit IgG	MolProbes	1 : 800	
	Hoechst	34580		Invitrogen	1 : 4000	Nuclei

Table 4.3: Chemicals

Name	Company
Agarose low gelling temperature	Sigma
ddH_2O	LifeTech/Invitrogen
Immunostain Enhancer	Pierce
Mounting Medium (Fluorescence)	DAKO
Normal Donkey Serum (NDS)	JIR/dianova
Paraformaldehyde (PFA)	Roth
Potassium chloride	Roth
Potassium phosphate	Sigma
Proteinase K	Roth
Sodium Chloride	Roth
Sodium hydrogen phosphate	Roth
Triton-X100	Merck/Roth/Sigma
Tween20	Roth/Sigma

4.2 Brain Sectioning

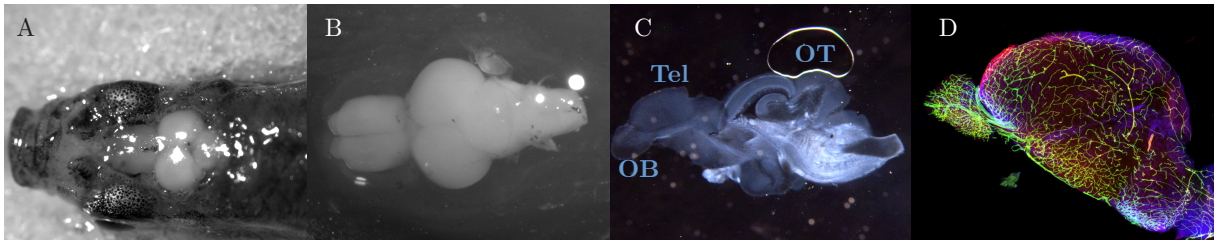

Figure 4.1: Brain Sectioning and Staining. Picture **A** demonstrates the opened skull during dissection. Picture **B** shows a brain that has been carefully removed. Images **C** and **D** display a 80 µm Vibratome section. Finally in a photo **D** final staining is represented.

1. First fish were killed and fixed with 4 % PFA.
2. Brains were carefully removed and washed in 1XPBS.
3. 4 % agarose was melt in a microwave and poured in a plastic container creating a first thin layer.

Table 4.4: Equipment and Software

Name	**Company**
Centrifuges	5424R, Eppendorf
Confocal microscope	Leica TCS SP8 MP
Dissection tools	FST
Falcons (15 mL/15 mL)	BD
Freezer, −20 °C	Liebher
Imaris 9.72	Oxford Instruments
Pasteur pipettes	Roth
Pipette tips	Sarstedt
Prism 8	GraphPad
Refrigerator, 4 °C	Liebher
Tubes (0.5 mL/15 mL)	Eppendorf
Vibratome	Leica

4. Afterwards brains were quickly dried with a paper towel and put on a half-dry agarose so they are flat and not deviating. This positioning allowed convenient sagittal sectioning.

5. Next second layer of agarose was poured over covering the samples.

6. When solid, a block was cut into smaller ones leaving more space on a side that would be glued to a platform.

7. Then a Vibratome was set up to 80 µm thickness and 40 $^{mm}/_{s}$ speed.

8. Afterwards agar block was sticked on the platform using super glue.

9. Lastly, sections were cut and transferred into well-plates with 1XPBS (1 well per 1 brain).

4.3 Staining

1. Brain sections were first incubated in blocking buffer (1XPBS + 0.3 % Triton-X100 + 10 % Normal Donkey Serum (NDS)) for 1 hour at RT with shake.

2. Afterwards they were incubated in the 1st antibody diluted in 4 parts of 1XPBS + 0.1 % Triton-X100 + 2 % NDS plus 1 part Immune Enhancer, overnight at 37 °C.
3. Samples were washed 5X for 10 min in 1XPBS + 0.1 % Tween20.
4. The next step was an incubation in the 2nd antibody with 4 parts of 1XPBS + 0.1 % Tween20 for 2 hours at 37 °C and 1 part Immune Enhancer, protected from light.
5. Then sections were washed 5X for 10 min in 1XPBS + 0.1 % Tween20.
6. Next they were washed once for 10 min in 1XPBS.
7. Afterwards samples were quickly washed in ddH_2O.
8. Finally they were carefully mounted on a cover slide with DAKO and then imaged.

4.4 Imaging

For the imaging Leica TCS SP8 multiphoton microscope was used. All the images were taken with 20X Objective.

4.5 Hybridization

One of the contributions was the hybridization protocol for Zebrafish brain that eventually worked really well.

First, Zebrafish brains were transferred into 12-well plate with basket inside in 100 % Methanol.

4.5.1 Rehydration

1. Samples were washed for 5 min in 75 % Methanol 25 % PBS.
2. Then for another 5 min in 50 % Methanol 50 % PBS.

3. And for another 5 min in 25 % Methanol 75 % PBS.

4. Finally they were washed 4× 5 min in 1XPBS.

4.5.2 Permeabilization

1. Samples were digested with proteinase K (20 µg/mL Proteinase K in PBS) for 20 min.

2. Afterwards they were washed 2× 5 min in 1XPBS.

4.5.3 Postfixation

1. Brains were washed in 4 % PFA/PBS for 20 min.

2. Next 5× 5 min in 1XPBS.

Afterwards samples were transferred in sterile single-packed 2 mL Eppendorf tubes.

4.5.4 Prehybridization

Probes were incubates in 1 mL of Hybridization Mix (HM) for 3 h.

4.5.5 Hybridization

1. HM was carefully removed from the samples.

2. 500 µL of *in situ* probe was added.

3. Brains were incubated at 70 °C overnight.

4.5.6 Preparation for day 2

1. Posthybridization solutions were prewarmed.

2. 12-well plate with posthybridization solutions was prepared.

3. Brains in the *in situ* probe liquid were placed into a clean 36 mm petri dish with a basket in it.

4. *In situ* probe liquid was carefully collected into the corresponding Eppendorf tube.

5. Baskets with brains were transferred in the previously prepared 12-well plate.

4.5.7 Posthybridization washes (performed at 70 °C)

- 10 min in 75 % HM 25 % 2× SSC.
- 10 min in 50 % HM 50 % 2× SSC.
- 10 min in 25 % HM 75 % 2× SSC.
- 10 min in 2× SSC.
- 2× 30 min in 0.2× SSC.

4.5.8 Preincubation washes (performed at room temperature (RT))

- 5 min in 75 % 0.2× SSC 25 % PBS.
- 5 min in 50 % 0.2× SSC 50 % PBS.
- 5 min in 25 % 0.2× SSC 75 % PBS.
- 5 min in 1XPBS.

4.5.9 Blocking and antibody incubation

1. Samples were blocked with 2 $^{mg}/_{mL}$ BSA, 5 % sheep serum in PBS for 2 h at RT.

2. Pax2a antibody was diluted 1:2000 in blocking buffer and incubated overnight.

4.5.10 Equilibration steps

1. First, brains were washed for 2 hours in 2 $^{mg}/_{mL}$ BSA in PBS.

2. Next they were washed 3× 5 min in a freshly prepared AP staining buffer.

4.5.11 Staining

1. Probes were transferred into a well filled with AP-Buffer.

2. Afterwards they were stained with NBT/BCIP (20 µL of the NBT/BCIP stock solution to 1 mL of AP-Buffer) on shaker protected from light for 3.5 h.

Samples were monitored every 30 min to prevent overstaining. Results are in the Appendix A.

Chapter 5

Results

In order to get a better understanding of the vessel development throughout the aging, our team had conducted experiments using 11- and 24-month old Zebrafish. For better vessel visualization we have used tg(kdrl:eGFP)^{s843} reporter line in younger animals and tg(kdrl:eGFP)^{s843}/tg(gata)1 : (dsRed)^{sd2} in older ones as they both highlight the vasculature with a green color. To investigate BBB properties we stained our brain sections with Claudin5. A major part of our project was imaging and in an effort to accomplish it, we used Leica TCS SP8 MP microscope along with Imaris 9.72 software to produce the following images. Finally, we performed statistical analysis using Prism 8 software where we compared the vessel density in young and aged species as well as evaluated the quality of BBB throughout the Zebrafish lifespan.

First component of our study is imaging. Figure 5.1 demonstrates Telencephalon and *Bulbus Olfactorius* of a young (11 m.o.) fish. To be able to evaluate brain vasculature we decided to use sagittal sections because of the prominent vessel that was used as a guideline to measure the density. These samples had already contained a GFP reporter line where endothelial cells appear green in the pictures 5.1A and E. In order to investigate BBB characteristics, samples were stained with Claudin5 for TJs that look red in images 5.1B and F. We have also used Hoechst to identify nuclei and in pictures 5.1C and G they look blue.

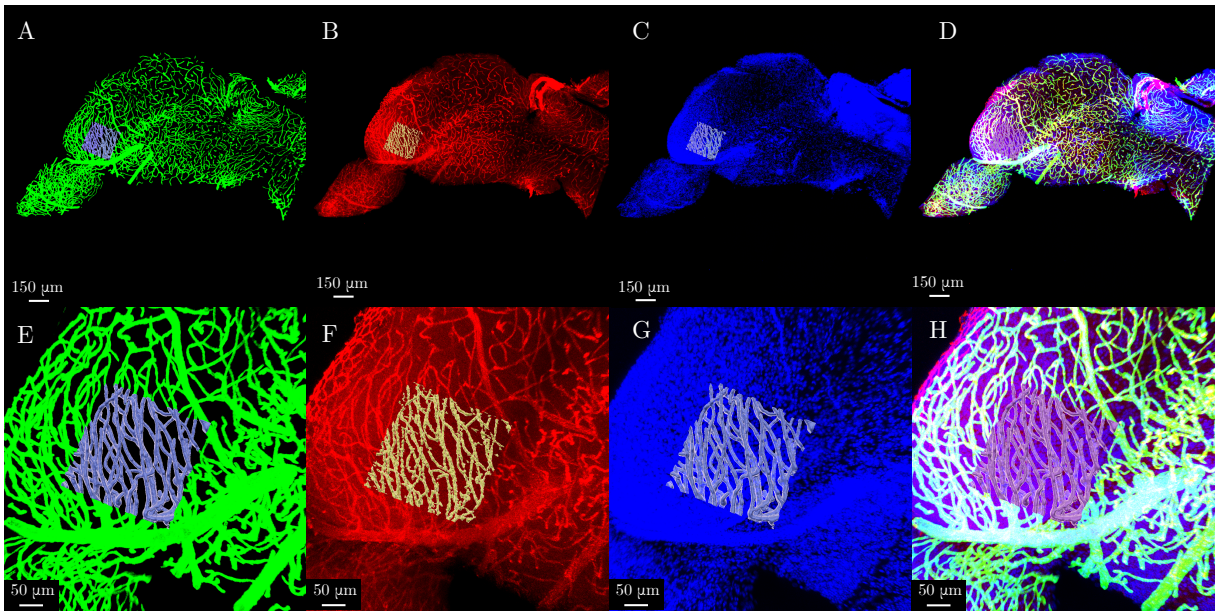

Figure 5.1: Telencephalon of 11 m.o. Zebrafish Confocal images of Telencephalon and *Bulbus Olfactorius*. Pictures **A**—**D** show overview images (Scale Bar 150 µm) while **E**—**H** demonstrate detailed version of the samples (Scale Bar 50 µm). Images **A** and **E** demonstrate vessels staining with eGFP (green), **B** and **F** — TJ staining with CLDN5 (red), **C** and **G** nuclei staining with Hoechst (blue). Pictures **D** and **H** represent merged channels. The colored squares are 300 µm by 300 µm in size and indicate the region that had been analyzed.

For a better visualization we first attempted to merge these three channels by using Fiji (ImageJ) program.

However, in a process of preparing figures, we concluded that snapshots made in Imaris 9.72 and merged together with Adobe Illustrator look way more representable as is noticeable in a Figure 5.1D and H. Top part of the figure, containing photos A–D, serves to give an overview (Scale Bar 150 µm) and the bottom part, with images E–H, reveals the important details and the main area of interest (Scale Bar 50 µm).

Figure 5.2 shows the same part of the brain of an older (24 m.o.) fish. The staining here is also the same as in younger ones: GFP (green) for vessels (images A and E), Claudin5 (red) for TJs (images B and F) and Hoechst (blue) for nuclei (images C and F). Pictures D and H show merged channels. Correspondingly, images A—D provide an overview and E—H display a region we focused on.

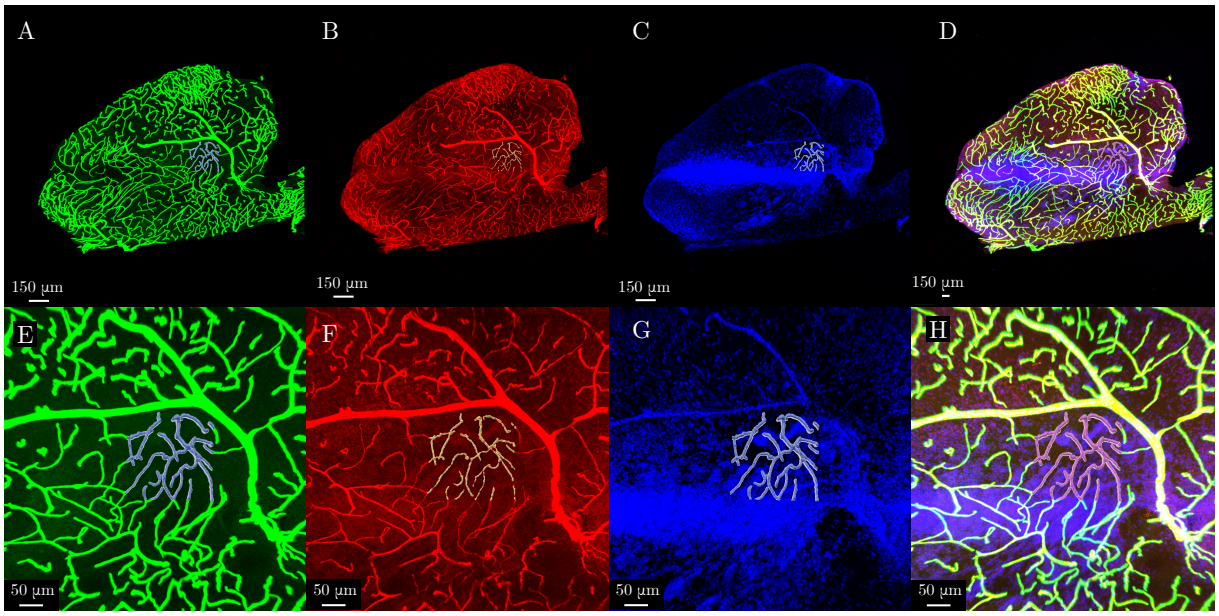

Figure 5.2: Telencephalon of 24 m.o. Zebrafish. Confocal images of Telencephalon and *Bulbus Olfactorius*. Pictures **A**—**D** show overview images (Scale Bar 150 µm) while **E**—**H** demonstrate detailed version of the samples (Scale Bar 50 µm). Images **A** and **E** demonstrate vessels staining with eGFP (green), **B** and **F** — TJ staining with CLDN5 (red), **C** and **G** nuclei staining with Hoechst (blue). Pictures **D** and **H** represent merged channels. The colored squares are 300 µm by 300 µm in size and indicate the region that had been analyzed.

The difference between Figures 5.1 and 5.2 is already visually noticeable. By comparing these two figures it is clear that the aged animals demonstrate decreased vessel density. Nonetheless, to substantiate our imaging results, further statistical analysis is required to make genuine statements.

For statistics we performed an unpaired t-test using Prism 8 Software that analyzed the data from Imaris where we chose a particular 300 µm by 300 µm area and measured number of tg(kdrl:eGFP)^{s843} and Claudin5 staining there. To get even more accurate results we removed 1–2 outliers from each group.

Figure 5.3A demonstrates the area of tg(kdrl:eGFP)^{s843} coverage in animals 11 and 24 months of age. In this plot we included 9 young fish and 7 old ones. It has been discovered that vessel density in 24-months old Zebrafish shows a significant ($p = 0.0093$) decrease when compared to 11-months old ones. $^{1.72 \cdot 10^5 \text{tg(kdrl:eGFP)}^{s843}}/_{\mu m^2}$ is the average for younger

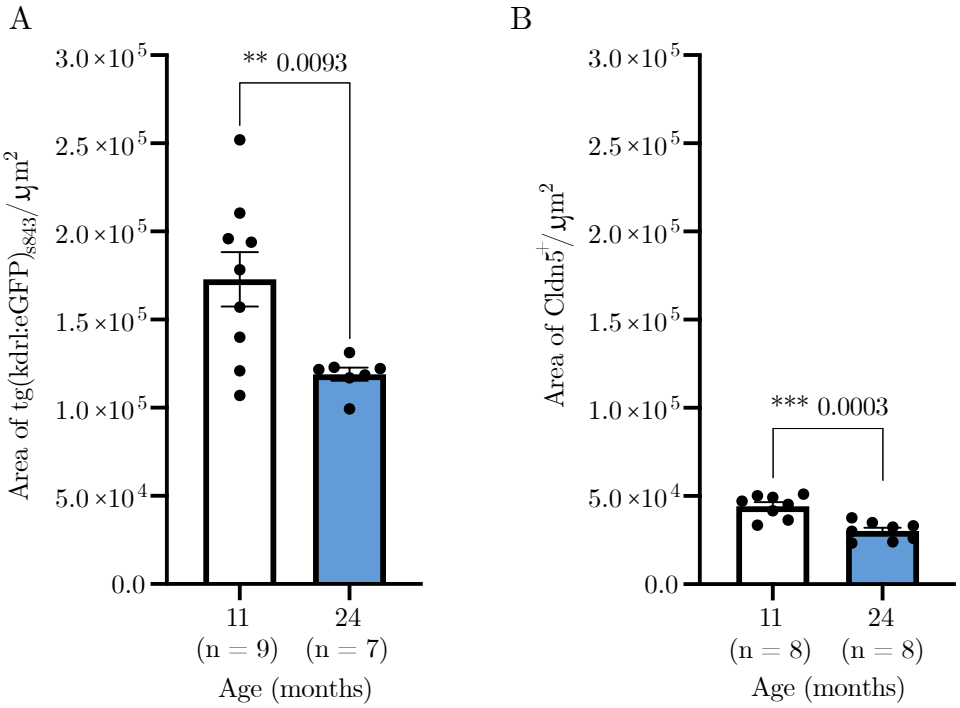

Figure 5.3: CLDN5 and Vessel Density. **A** An unpaired t-test for the density of CLDN5 on 300 × 300 µm^2 area. **B** An unpaired t-test for the tg(kdrl:eGFP)^{s843} density on 300 × 300 µm area. All outliers had been removed for more accurate results.

species and from the Figure 5.4A and C it is clear that a coverage is really high. Older fish, however, have a mean of only $^{1.19\cdot10^5\text{tg(kdrl:eGFP)}^{s843}}/_{\mu m^2}$ and images 5.4B and D show that during senescence vessel density is decreased according to our findings seen between 11- and 24- months old fish.

Plot 5.3B, displays the area of Claudin5-positive area in 11- and 24-months old species. For this part we chose 8 young and 8 old animals. The statistical analysis revealed that the difference between them is indeed significant (p = 0.0003). 11-months old animals possess the average of $^{4.43\cdot10^4\text{CLDN}^+}/_{\mu m^2}$ in comparison to 24-months old ones with $^{3.00\cdot10^4\text{CLDN}^+}/_{\mu m^2}$ mean. Images 5.4A and C compared to pictures 5.4B and D also visually reaffirm statistical data demonstrating the smaller area of coverage and fewer Claudin5 in aged brain.

Changes in vessel and Claudin5 density are also detectable in pictures 5.1A, B, E and F and Figure 5.2A, B, E and F. This finding suggests that brain perfusion might worsen with age. It also correlates well with recent discoveries that will be discussed further.

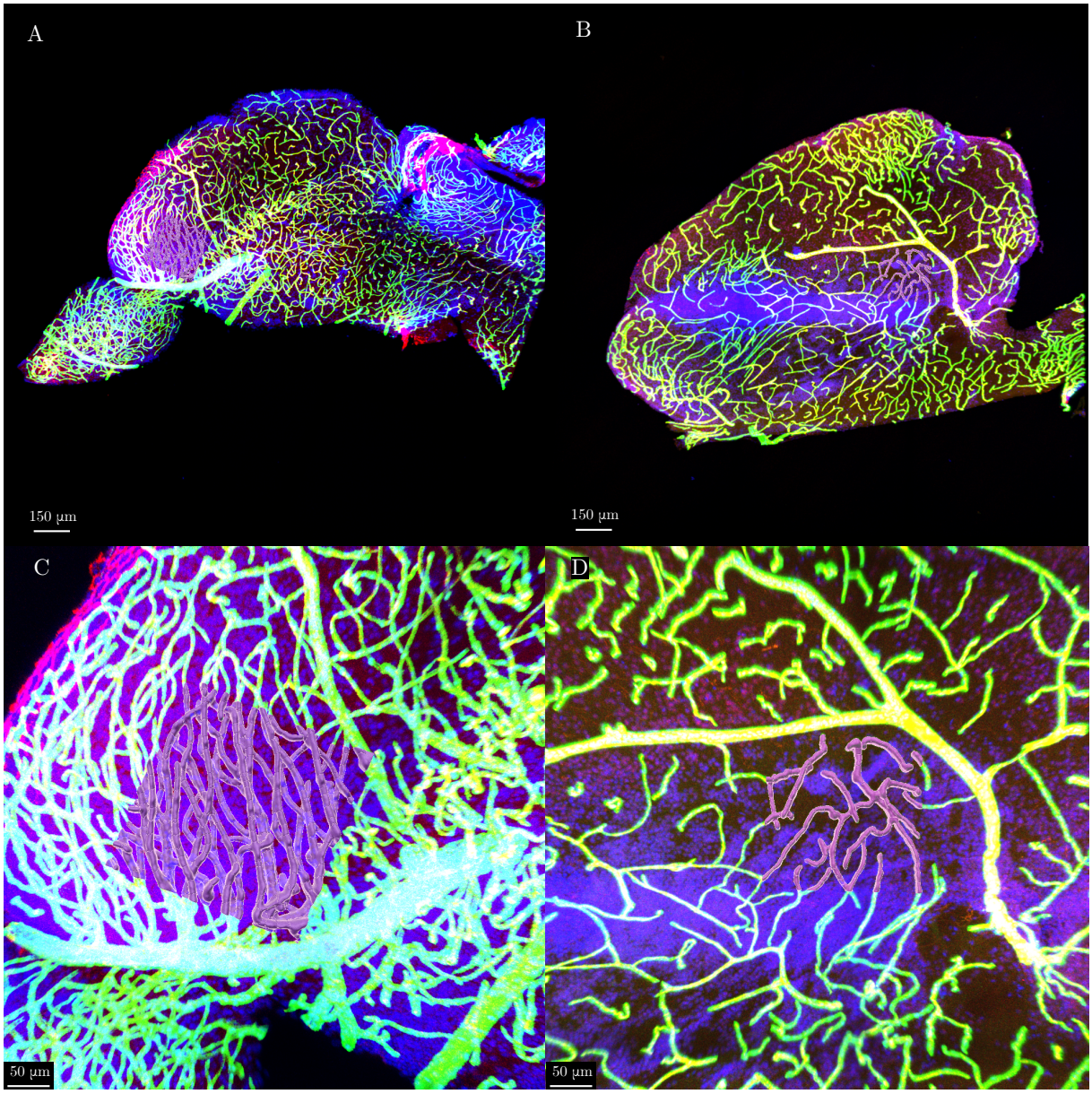

Figure 5.4: CLDN5 and Vessel Density Imaris Images. Here all 3 channels (Vessel, Claudin and Hoechst) were merged for a better visual representation of the plots. Images **A** and **C** show a brain of 11 m.o. Zebrafish, where picture **A** is an overview one and picture **C** provides detailed outlook. Graphics **B** and **D** show Telencephalon of an aged 24 m.o. fish. Again top picture **B** provides more general perspective (Scale Bar 150 µm), while the bottom **D** manifests a detailed view (Scale Bar 50 µm). The coverage here can be seen as Vessel (green) and Claudin (red) channels merged together, thus appear light orange in this picture. Colored squares are 300 µm by 300 µm in size and represent the analyzed region.

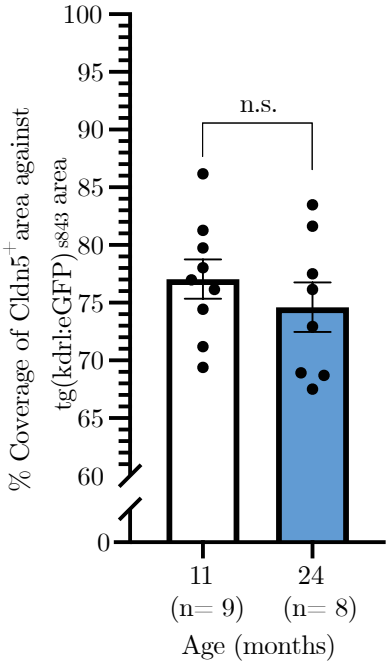

Figure 5.5: CLDN5 Coverage. Unpaired t-test for the coverage percentile of CLDN5 against tg(kdrl:eGFP)^{s843} area. All outliers had been removed for more accurate results.

Our second idea was to evaluate the percentage of Claudin5 coverage against the tg(kdrl:eGFP)^{s843} reporter line on the same area in order to investigate the change in properties of BBB throughout the aging. Figure 5.8A–D displays merged tg(kdrl:eGFP)^{s843} and Claudin5 images for visual representation. It is, however, hard to undoubtedly claim a change in this protein's expression. Plot 5.5, on the other hand, shows that a difference between younger (11 m.o.) and older (24 m.o.) animals is insignificant ($p > 0.05$) in this case. There is, nonetheless, a clear decreasing tendency while the mean for 11-months old fish equals 77.00 % and for 24-months old species this number is 74.61 %.

Interestingly, this result perfectly substantiated the gradual aging hypothesis. It is also especially useful to compare images in a Figure 5.6 that show a drastic decline in vessel density at 24 months with the pictures in a Figure 5.7. What is important is to understand that even though older fish have fewer vessels, their quality and permeability of BBB are still relatively good, thus we may claim that we now have a clear evidence that within Zebrafish aging occurs indeed gradually like in mammals.

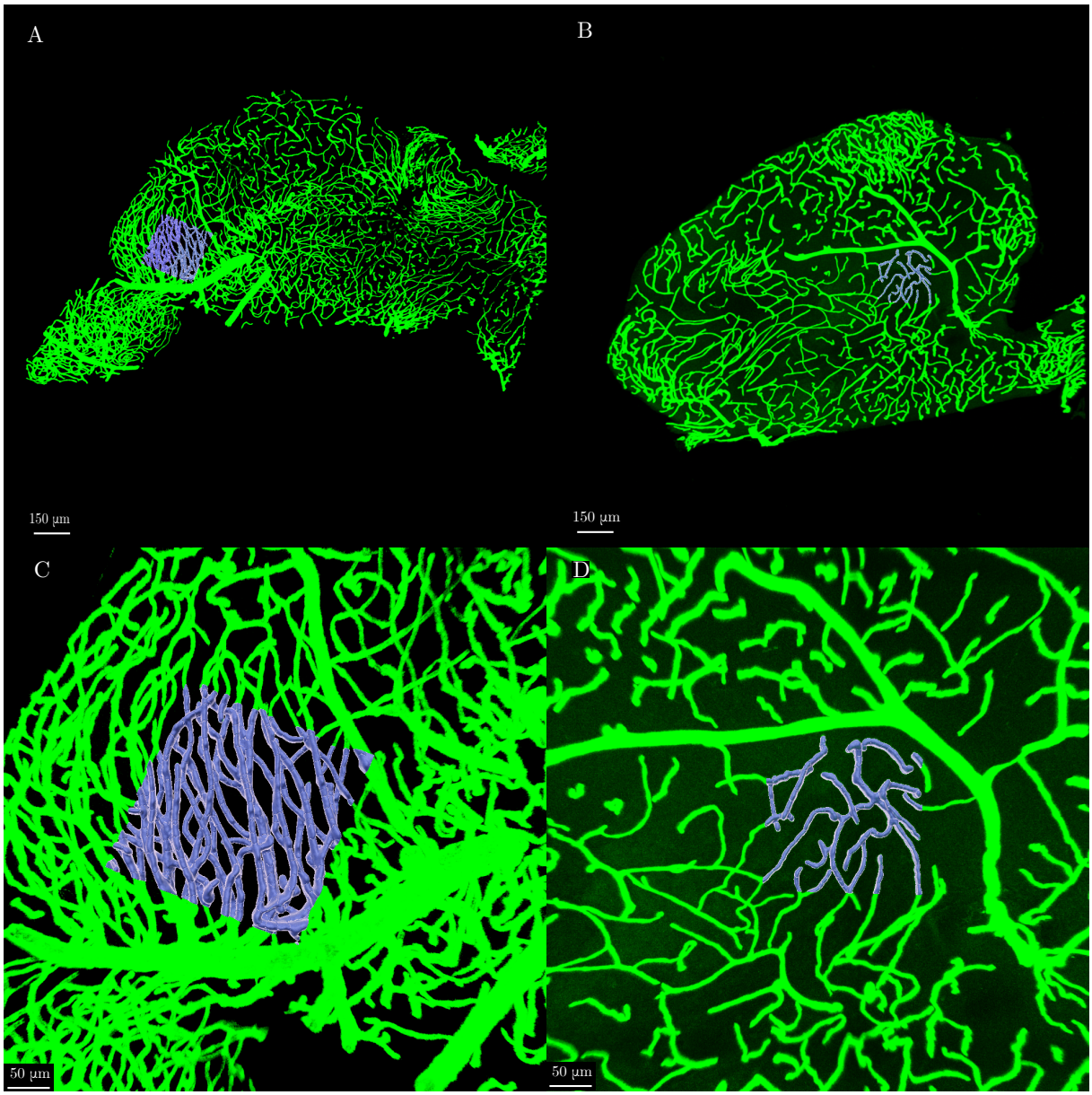

Figure 5.6: tg(kdrl:eGFP)^{s843} Coverage Imaris Images. In order to better understand the vessel coverage and density, we combined young and aging sections of tg(kdrl:eGFP)^{s843}. As usual, the top layer displays an overview (Scale Bar 150 µm), while the bottom one shows detailed regions (Scale Bar 50 µm). Pictures **A** and **C** represent a young 11-months old animal with an extremely high vessel density and tg(kdrl:eGFP)^{s843} coverage. Images **B** and **D**, on the other hand, reveal diminished number of vessels in older, 24-months old, species. Colored squares are 300 µm by 300 µm in size and display the region of interest.

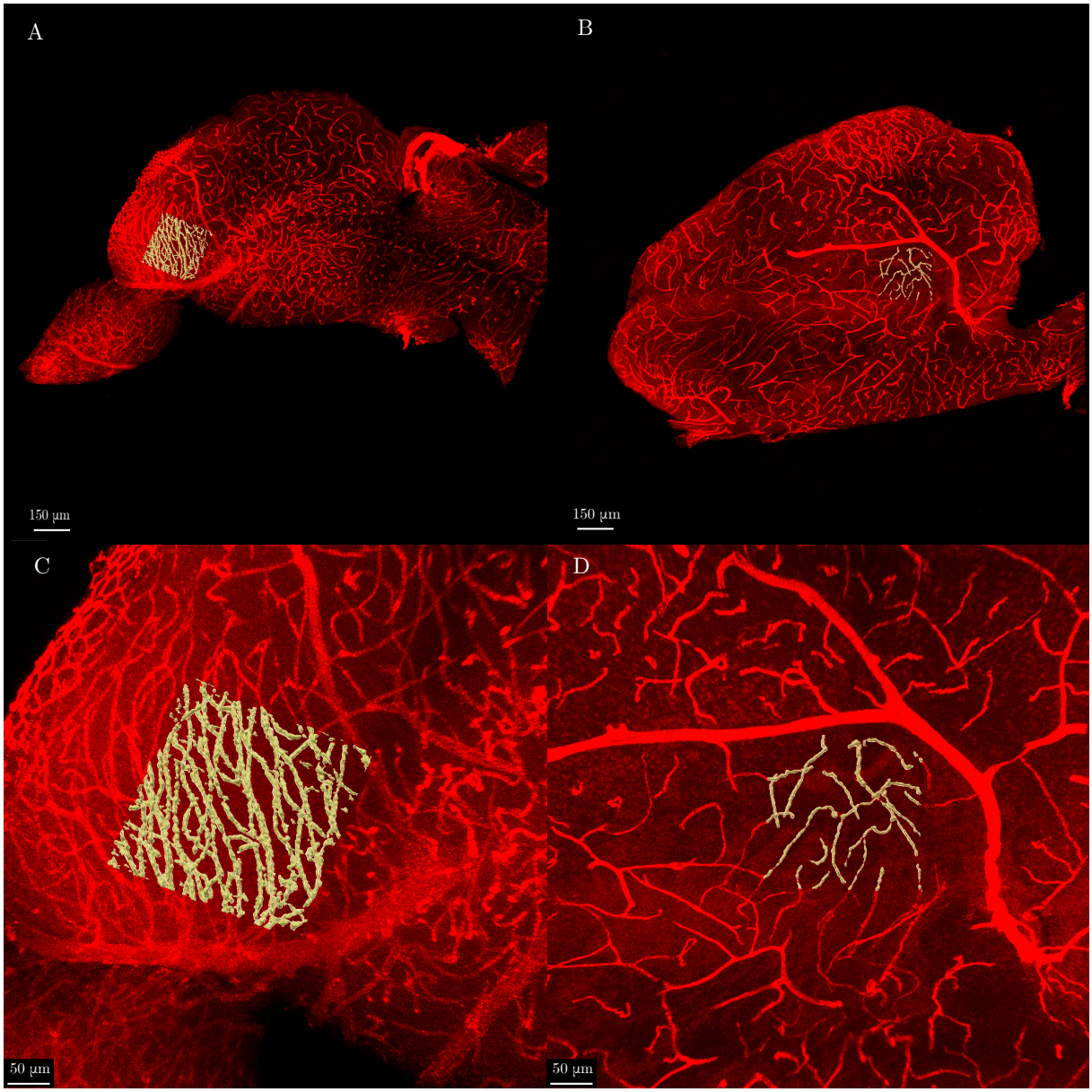

Figure 5.7: CLDN5 Coverage Imaris Images. To investigate the coverage of Claudin5, we combined young and aging sections of $CLDN^+$ area. As usual, the top layer displays an overview (Scale Bar 150 µm), while the bottom one shows detailed regions (Scale Bar 50 µm). Pictures **A** and **C** represent a young 11-months old animal with high Claudin5 coverage. Images **B** and **D**, on the other hand, reveal diminished amount of TJs in older, 24-months old, species. Colored squares are 300 µm by 300 µm in size and display the region of interest.

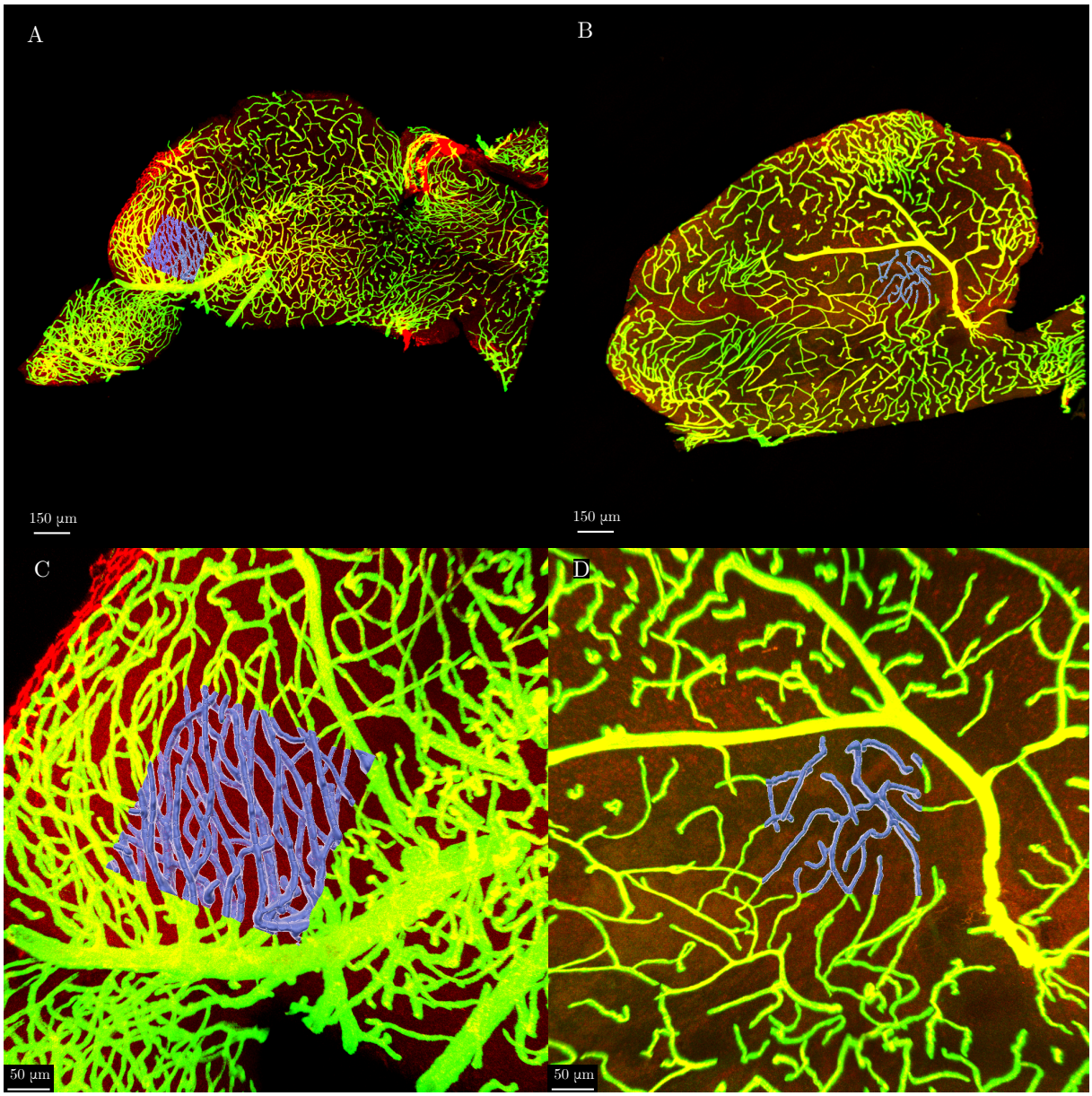

Figure 5.8: CLDN5 Coverage Merged Imaris Images. Here we merged Vessel and Claudin5 channels for easier recognition of the changes in Claudin5 expression. Images **A** and **C** show a brain of 11 m.o. Zebrafish, where picture **A** is an overview one (Scale Bar 150 µm) and picture **C** provides detailed outlook (Scale Bar 50 µm). Graphics **B** and **D** show Telencephalon of an aged 24 m.o. fish. The coverage here can be seen as Vessel (green) and Claudin (red) channels merged together, thus appear light orange in this picture. Again top picture **B** provides more general perspective (Scale Bar 150 µm), while the bottom **D** manifests a detailed view (Scale Bar 50 µm). Colored squares are 300 µm by 300 µm in size and represent analyzed region.

Chapter 6

Discussion

6.1 Does aging in Zebrafish occur gradually like in mammals?

Our first question was if aging in Zebrafish occurs at the same pace as in mammals.

The first paper to mention gradual aging in Zebrafish was the one by Kishi et al. (2009) who observed a slow retinal atrophy in Zebrafish between the ages of 20 and 58 months. In their experiments authors investigated liver and retinal tissues throughout the age. For the liver part they chose 1-, 2.1-, 2.8-, and 3.8-year old animals. In histological sections stained with Hematoxylin and eosin (HE) or Periodic Acid-Schiff (PAS) they have noticed an increased hepatocyte density and the biomarker in aging liver tissue and aging pigment — lipofuscin. For eye sections fish 5-, 20-, 36-, and 58-month of age were stained with HE and investigated. Compared to 20-months-old, 58-month-old animals demonstrated increased "drusen-like accruals" with an autofluorescence in the retinal pigment epithelium. These changes appear to be similar to those seen in age-related macular degeneration (AMD) in humans. Authors also mentioned their personal observation that almost all aged Zebrafish developed cataracts by 4 years of age.

The second idea was revealed by Shimoda et al. (2014). Age-related changes in DNA methylation which is a criterion for the fundamental cause of senescence had been investi-

gated earlier in mammals. Therefore, authors conducted this study to figure out whether the same process occurs in vertebrates. For analysis they used extracted genomic DNA from the sperm, 2-day post fertilization embryos, and muscle of 3-, 18-, and 30-month-old fish. The choice of muscle cells was conditioned by the fact that it is a predominant structure of the fish species, thus, an adequate representative of somatic cells.

It turned out that Zebrafish genome, which is highly methylated at first, gradually and clearly loses methylcytosine in somatic cells. Moreover, age-dependent hypomethylation preferentially occurred at the CpG island shore domain, which is associated with vertebrates' genes and has been hypomethylated in aging humans as well. In male germ cells, on the other hand, methylcytosine was not decreased with aging.

Lastly, Manuel et al. (2015) decided to use an inhibitory avoidance paradigm to assess the mechanisms underlying learning and memory formation in Zebrafish. They have raised animals in an environmentally enriched tank that led to the decreased anxiety-like behavior and increased exploration in these animals. Inhibitory avoidance was also greatly reduced in species 6- and 12-month of age. The authors also reported that telencephalic mRNA levels of genes related to plasticity and learning, such as proliferating cell nuclear antigen (*pcna*), neurogenic differentiation (*neurod*), cocaine- and amphetamine-regulated transcript 4 (*cart4*) and cannabinoid receptor 1 (*cnr1*) were lower in enriched-housed fish, while the ratios of mineralocorticoid receptor (*nr3c2*) to glucocorticoid receptor α (*nr3c1(α)*) and glucocorticoid receptor β (*nr3c1(β)*) to glucocorticoid receptor α (*nr3c1(α)*) were higher. 24-months-old fish, on the other hand, displayed a delayed inhibitory avoidance and reduced expression of aforementioned neuroplasticity genes.

Our experiments are the first ones to be performed on Zebrafish brain vessels. The fact that the levels of Claudin5 coverage against tg(kdrl:eGFP)^{s843} density were not significantly decreased gives us the reason to think that the properties of BBB will decline slowly. Certainly, further experiments using older animals are crucial to prove this theory,

nonetheless, our current results substantiate the overall hypothesis about gradual aging in Zebrafish.

6.2 What happens to BBB during aging?

Blood-brain barrier during aging is especially important topic since the majority of neurodegenerative disorders are associated exactly with BBB impairment. Unfortunately, there are no BBB studies in aging Zebrafish, therefore we can only compare our findings with ones performed on humans or mice.

He et al. (2014) presumed that the changes of the BBB may be the cause of many pathophysiological processes in the brain of subjects with chronic sleep restriction (CSR). To mimic an actual CSR mice used for the study underwent 6 consecutive days of CSR in the sleep deprivation cages fabricated by Pinnacle Technology. Two groups of cerebral microvessels were compared to investigate the effect of CSR on TJ expression: naive ones and those from mice after 6 days of CSR. The results showed that in the CSR group, there was reduction of mRNAs of TJs proteins such as occludin, claudin-1, claudin-5, and ZO-2. "The immunofluorescence of occludin was lost in most areas of the vessels in the CSR mice, and the remaining intensity was dramatically decreased in patchy areas."

BBB permeability was also significantly disturbed: during the study of the brain uptake of sodium fluorescein 10 min after intravenous injection, it has been revealed that CSR mice demonstrated an increased uptake of sodium fluorescein in cerebral cortex, subcortical region, brain stem, and cerebellum. The uptake in total brain also had been increased in CSR mice compared to the control group. These results indicate that CSR resulted in an increase of paracellular permeability of the BBB.

Another work conducted by Montagne et al. (2015) used an advanced dynamic contrast-enhanced MRI protocol with post-processing analysis with an improved spatial and temporal resolutions for the regional BBB permeability quantifying in the living human brain. In participants with no cognitive impairment (NCI) and with mild cognitive impairment

(MCI) they investigated 12 CNS regions including hippocampus, CA1, CA3, dentate gyrus (DG) as well as different cortical and subcortical (e.g., thalamus, striatum, and caudate nucleus). Authors also observed white matter regions including *corpus callosum* and internal capsule.

Interestingly, it has been found that NCI individuals had an age-dependent progressive loss of BBB integrity in the hippocampus area, while in cortical and subcortical areas no changes had been discovered. Subcortical white matter fibers, corpus callosum, and internal capsule also did not show any age-related changes in BBB permeability. Therefore, authors suggested that early vascular leakage in the aging human brain might begin in the hippocampus, which normally displays the highest barrier properties. In MCI individuals the BBB disruption was more prominent than in the age-matched neurologically intact controls. Thus, it might be logical to conclude that there is a possibility that it may play a role in early cognitive impairment.

In our work we have yet to find out the implications of BBB disruption in Zebrafish model. Although, in our case the decline in Claudin5 expression was not yet significant, we anticipate that in animals older than 24 months we might see more drastic BBB breakdown.

6.3 Does aging affect vessel density?

Another important point was to assess whether aging process affects vessel density. Again there are no studies done on Zebrafish; we, however, found the most relevant works performed on humans and mice.

First project by Lin et al. (2019) was conducted to determine whether the age-related alterations occur in the retinal tissue perfusion (RTP) and volumetric vessel density (VVD) in healthy subjects. For this purpose they divided 148 healthy subjects (age 18 to 83 years) into four groups: G1 $<$ 35 years; G2 35–49 years; G3 50–64 years; and G4 $>$ 65 years, and measured their RTP and VVD at the macula. It has been established

that RTP and VVD of the retinal vascular network and deep vascular plexus (DVP) reached a peak in G2 group and then were negatively affected by age.

This study is the first one to demonstrate the age-related alterations in the RTP and VVD during normal aging in a healthy population. The authors concluded that the decreased RTP and VVD in the DVP along with increased VVD in the SVP might be a characteristic pattern of normal aging in the healthy population.

The most recent work in this area has been done by Chen et al. (2021). They generated cell-cell interactome and 3D spatial proteomic data by performing deep imaging of whole glands at a single-cell resolution comparative to understand age-related perturbations of the EC compartment in endocrine glands in humans and mice. It has been revealed that the testis, thyroid gland and pancreas demonstrated the most prominent decline in a microvascular density associated with aging. These organs also showed a significant age-related decline in artery numbers. To prove these age-related changes in microvascular density and arterial numbers in testis, pancreas and thyroid gland, they were compared to the adult and aged mice.

The data we got in our project clearly show the same patterns: correspondingly to mice and humans, vessel density decreases drastically in 24-months old Zebrafish which is another big advantage of it as a model organism.

Summarizing all aforementioned, we came to the conclusion that our results show a great correlation with the literature. Keeping in mind that we are the first to investigate vessel density and BBB properties within aging Zebrafish, such parallels suggest further perspectives in the studying of senescence. Furthermore, the discovery of yet another evidence for the gradual aging hypothesis provides even more opportunities for this model organism.

Chapter 7

Further Study

Finally we want to propose several ideas for further study:

1. Although the results we acquired in our work are promising, we suggest performing the same experiments on animals older than 24 month. Realistically, 30–36-months old fish might be suitable to further confirm our findings. It would also be interesting to see at what point of time neurodegeneration will occur.

2. Following the topic of neurodegeneration, it might be beneficial to perform staining on radial glia and microglia to see if the loss of vessel density contribute to neural damages.

3. Our next suggestion is to stain other organs. In our opinion, particularly important organ would be heart due to the number of heart pathologies that are associated with age. We have already made an effort to try several methods to stain heart, however, neither worked perfectly. Our attempts are described in Appendix B.

4. Another idea is to investigate molecular players in knock-out animals to see whether there are changes throughout aging. Recent study by Erbaba et al. (2020) revealed several molecules that are critical for brain aging such as: Activated leukocyte cell adhesion molecule (ALCAM), CLDN19, T-Cell Immunoglobulin and Mucin Do-

main Containing 4 (timd4), Connexin 47 (cx47), Neural cell adhesion molecule L1.2 (NADL1.2), Myelin-associated glycoprotein (MAG) and Neurofascin (NFASCA).

5. Paper by Castranova et al. (2021) also revealed a possibility to perform live imaging of Zebrafish intracranial lymphatics by using Casper genetic background to eliminate melanocyte and iridophore cell populations making the scull transparent, thus increasing the clarity.

6. Finally, it may be interesting to investigate aging through another novel model organism such as the African turquoise killifish (*Nothobranchius furzeri*). It is known that this animal has the shortest lifespan among the aquarium fish, only about 3–6 months (Harel et al., 2015) and reaches sexual maturation already at 3–4 weeks (Kim et al., 2016). Thus it might be extremely useful to try this animal for further research.

Appendix A

in-situ Hybridization

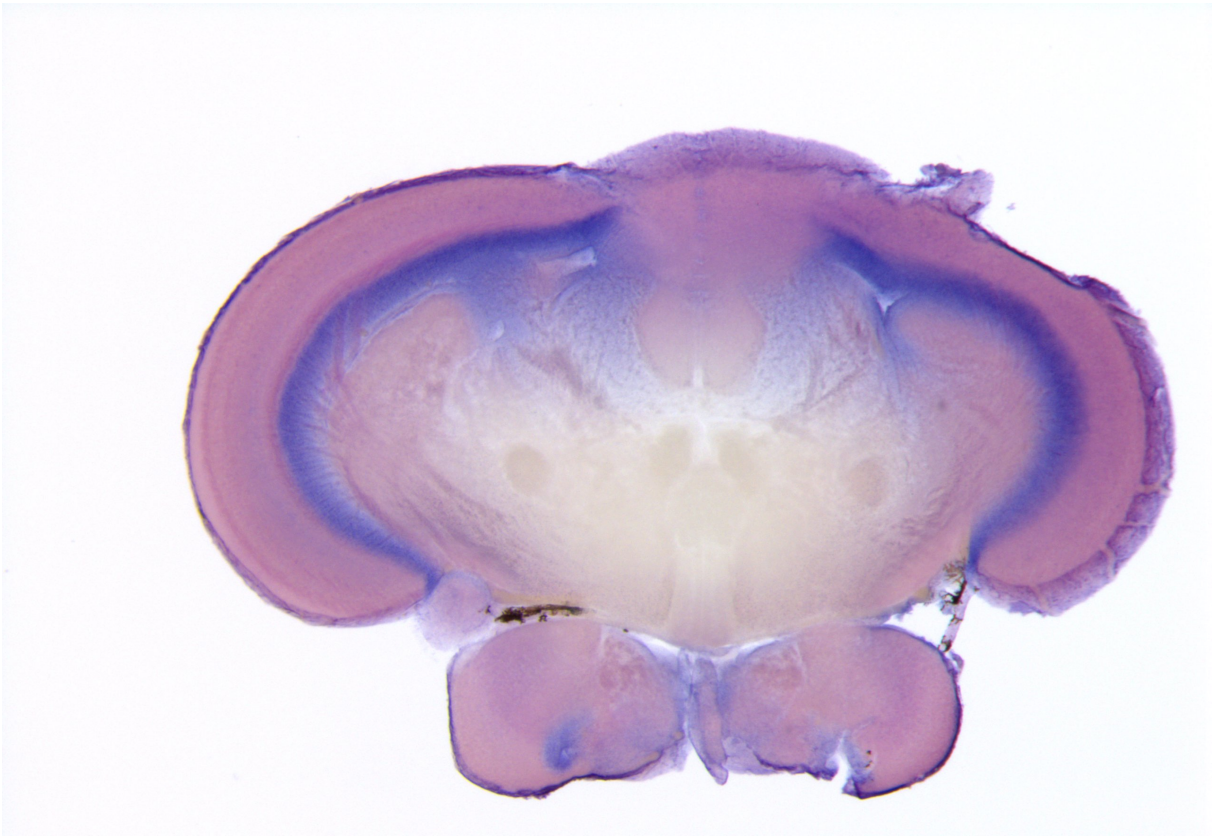

Figure A.1: *in situ* Hybridization Midbrain. Protocol and sectioning performed by Helene Juul Belling on a WT fish for Neuropilin A project.

Appendix B

Heart Staining Protocol

In this section we would like to elaborate on methods that had been used to perform heart staining and discuss the difficulties we have faced. Although they did not came out as successful as ones with brain sections we believe that the protocols we used might be helpful for further studies.

As shown in a Figure B.1 the staining appears almost fine on a border, it could not, however, properly penetrate all of the tissue. Interestingly, Hoechst nevertheless worked well. In a process we have tried sections ranging from 50 µm to 120 µm in thickness an all of them gave the same result. Tables B.1 and B.2 display different antibodies and their dilutions that we attempted. We also modified Tris-EDTA Buffer Antigen Retrieval

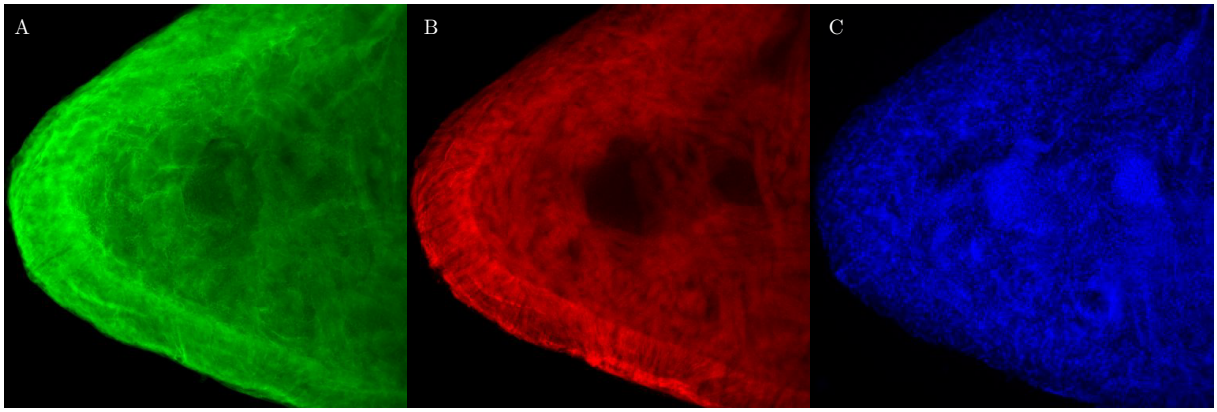

Figure B.1: Heart Staining. For this experiment Zebrafish heart was stained with MF20 (green), Huc (red) and Hoechst (blue) for nuclei.

Protocol with pH 9 and Citrate Buffer Antigen Retrieval Protocol with pH 6 as well as tested different temperatures (95 °C for pH 9 and 75 °C for pH 6). Finally, we inspected different incubation times.

B.1 Tris-EDTA Buffer Antigen Retrieval Protocol (pH 9)

The first protocol we tried to modify in order to get clearer images was Tris-EDTA Buffer Antigen Retrieval Protocol that has pH 9.

1. First a water bath was preheated with Eppendorf tubes with Tris-EDTA Buffer until 95 °C.
2. Then heart sections were immersed in the tubes and incubated for 20 min.
3. The water bath was turned off and the tubes were removed to cool down at a RT for another 20 min.
4. Afterwards sections were washed 2X for 3 min in ddH_2O.
5. Lastly samples were washed with 1XPBS 2X for 3 min and original staining protocol was continued.

B.2 Citrate Buffer Antigen Retrieval Protocol (pH 6)

Next protocol was the Citrate Buffer Antigen Retrieval one with pH 6. Here we proceeded with lower temperature of 75 °C and longer incubation time of 2 days.

1. First a water bath was preheated with Eppendorf tubes with 1.8 mL of Citrate Buffer until 75 °C.
2. Then heart sections were immersed in the tubes and incubated for 30 min.

3. The water bath was turned off and the tubes were removed and transferred into 12-well plate along with Citrate Buffer to cool down at a RT for 15 min.

4. Afterwards sections were washed 2X for 3 min in ddH_2O.

5. Lastly samples were washed once with 1XPBS for 3 min and original staining protocol was continued.

Table B.1: Antibodies for Tris-EDTA Buffer Antigen Retrieval Protocol

	Name	**Host**	**Clone**	**Company**	**Dilution**	**Staining**
1 AB Plate 1	FLI1	Rabbit	monoclonal	Abcam	1 : 400	Vessels
	Acetylated Tubulin	Mouse	6-11B-1	Sigma	1 : 200	Filaments
1 AB Plate 2	HUC	Rabbit	polyclonal	Abcam	1 : 400	Vessels
	MF20	Mouse	monoclonal	DSHB	1 : 200	Filaments
			Antigen			
2 AB Plate 1	Alexa_647	Donkey	anti-rabbit IgG	MolProbes	1 : 400	
	Alexa_555	Donkey	anti-mouse IgG	MolProbes	1 : 400	
2 AB Plate 2	Alexa_647	Donkey	anti-rabbit IgG	MolProbes	1 : 400	
	Alexa_555	Donkey	anti-mouse IgG	MolProbes	1 : 400	
	Hoechst	34580		Invitrogen	1 : 2000	Nuclei

Table B.2: Antibodies for Citrate Buffer Antigen Retrieval Protocol

	Name	**Host**	**Clone**	**Company**	**Dilution**	**Staining**
Primary Well-Plate 1	FLI1	Rabbit	monoclonal	Abcam	1 : 200	Vessels
	Acetylated Tubulin	Mouse	6-11B-1	Sigma	1 : 50	Filaments
Primary Well-Plate 2	HUC	Rabbit	polyclonal	Abcam	1 : 200	Vessels
	MF20	Mouse	monoclonal	DSHB	1 : 50	Filaments
			Antigen			
Secondary Well-Plate 1	Alexa_647	Donkey	anti-rabbit IgG	MolProbes	1 : 100	
	Alexa_555	Donkey	anti-mouse IgG	MolProbes	1 : 100	
Secondary Well-Plate 2	Alexa_647	Donkey	anti-rabbit IgG	MolProbes	1 : 100	
	Alexa_555	Donkey	anti-mouse IgG	MolProbes	1 : 100	
	Hoechst	34580		Invitrogen	1 : 2000	Nuclei

Bibliography

Amasheh, S., Dullat, S., Fromm, M., Schulzke, J. D., Buhr, H. J., & Kroesen, A. J. (2009). Inflamed pouch mucosa possesses altered tight junctions indicating recurrence of inflammatory bowel disease. *International Journal of Colorectal Disease*, *24*, 1149. doi:10.1007/s00384-009-0737-8.

Asnani, A., & Peterson, R. T. (2014). The zebrafish as a tool to identify novel therapies for human cardiovascular disease. *Disease Models & Mechanisms*, *7*, 763–767. doi:10.1242/dmm.016170.

Baker, D. J., & Petersen, R. C. (2018). Cellular senescence in brain aging and neurodegenerative diseases: evidence and perspectives. *The Journal of Clinical Investigation*, *128*, 1208–1216. doi:10.1172/JCI95145.

Banks, W. A., Kovac, A., & Morofuji, Y. (2018). Neurovascular unit crosstalk: Pericytes and astrocytes modify cytokine secretion patterns of brain endothelial cells. *Journal of cerebral blood flow and metabolism : official journal of the International Society of Cerebral Blood Flow and Metabolism*, *38*, 1104–1118. doi:10.1177/0271678X17740793.

Banks, W. A., Reed, M. J., Logsdon, A. F., Rhea, E. M., & Erickson, M. A. (2021). Healthy aging and the blood–brain barrier. *Nature Aging*, *1*, 243–254. doi:10.1038/s43587-021-00043-5.

Brown, L. S., Foster, C. G., Courtney, J.-M., King, N. E., Howells, D. W., & Sutherland, B. A. (2019). Pericytes and neurovascular function in the healthy and diseased brain. *Frontiers in Cellular Neuroscience*, *13*, 282. doi:10.3389/fncel.2019.00282.

Brunner, N., Stein, L., Cornelius, V., Knittel, R., Fallier-Becker, P., & Amasheh, S. (2020). Blood-brain barrier protein claudin-5 expressed in paired xenopus laevis oocytes mediates cell-cell interaction. *Frontiers in Physiology*, *11*, 857. doi:10.3389/fphys.2020.00857.

Budni, J., Bellettini-Santos, T., Mina, F., Garcez, M. L., & Zugno, A. I. (2015). The involvement of bdnf, ngf and gdnf in aging and alzheimer's disease. *Aging and disease*, *6*, 331–341.

Cai, W., Zhang, K., Li, P., Zhu, L., Xu, J., Yang, B., Hu, X., Lu, Z., & Chen, J. (2017). Dysfunction of the neurovascular unit in ischemic stroke and neurodegenerative diseases: An aging effect. *Ageing Research Reviews*, *34*, 77–87. doi:10.1016/j.arr.2016.09.006.

Castranova, D., Samasa, B., Galanternik, M. V., Jung, H. M., Pham, V. N., & Weinstein, B. M. (2021). Live imaging of intracranial lymphatics in the zebrafish. *Circulation Research*, *128*, 42–58. doi:10.1161/CIRCRESAHA.120.317372.

Chen, J., Lippo, L., Labella, R., Tan, S. L., Marsden, B. D., Dustin, M. L., Ramasamy, S. K., & Kusumbe, A. P. (2021). Decreased blood vessel density and endothelial cell subset dynamics during ageing of the endocrine system. *The EMBO Journal*, *40*, e105242. doi:10.15252/embj.2020105242.

Crous-Bou, M., Minguillón, C., Gramunt, N., & Molinuevo, J. L. (2017). Alzheimer's disease prevention: from risk factors to early intervention. *Alzheimer's Research & Therapy*, *9*, 71. doi:10.1186/s13195-017-0297-z.

Dalkara, T., Gursoy-Ozdemir, Y., & Yemisci, M. (2011). Brain microvascular pericytes in health and disease. *Acta Neuropathologica*, *122*, 1. doi:10.1007/s00401-011-0847-6.

Daneman, R., & Prat, A. (2015). The blood–brain barrier. *Cold Spring Harbor Perspectives in Biology*, *7*, a020412. doi:10.1101/cshperspect.a020412.

Edelmann, K., Glashauser, L., Sprungala, S., Hesl, B., Fritschle, M., Ninkovic, J., Godinho, L., & Chapouton, P. (2013). Increased radial glia quiescence, decreased reactivation upon injury and unaltered neuroblast behavior underlie decreased neurogenesis in the aging zebrafish telencephalon. *Journal of Comparative Neurology*, *521*, 3099–3115. doi:10.1002/cne.23347.

Erbaba, B., Burhan, Ö. P., Serifoglu, N., Muratoglu, B., Kahveci, F., Adams, M. M., & Arslan-Ergül, A. (2020). Zebrafish brain rna sequencing reveals that cell adhesion molecules are critical in brain aging. *Neurobiology of Aging*, *94*, 164–175. doi:10.1016/j.neurobiolaging.2020.04.017.

Florian, P., Amasheh, S., Lessidrensky, M., Todt, I., Bloedow, A., Ernst, A., Fromm, M., & Gitter, A. (2003). Claudins in the tight junctions of stria vascularis marginal cells. *Biochemical and Biophysical Research Communications*, *304*, 5–10. doi:10.1016/S0006-291X(03)00498-4.

Furuse, M. (2010). Chapter 1 - introduction: Claudins, tight junctions, and the paracellular barrier. (pp. 1–19). Academic Press volume 65 of *Current Topics in Membranes*. doi:10.1016/S1063-5823(10)65001-6.

Furuse, M., Hata, M., Furuse, K., Yoshida, Y., Haratake, A., Sugitani, Y., Noda, T., Kubo, A., & Tsukita, S. (2002). Claudin-based tight junctions are crucial for the mammalian epidermal barrier : a lesson from claudin-1-deficient mice . *Journal of Cell Biology*, *156*, 1099–1111. doi:10.1083/jcb.200110122.

Furuse, M., Hirase, T., Itoh, M., Nagafuchi, A., Yonemura, S., Tsukita, S., & Tsukita, S. (1993). Occludin: a novel integral membrane protein localizing at tight junctions. *Journal of Cell Biology*, *123*, 1777–1788. doi:10.1083/jcb.123.6.1777.

Greene, C., Hanley, N., & Campbell, M. (2019). Claudin-5: gatekeeper of neurological function. *Fluids and Barriers of the CNS*, *16*, 3. doi:10.1186/s12987-019-0123-z.

Günzel, D., Amasheh, S., Pfaffenbach, S., Richter, J. F., Kausalya, P. J., Hunziker, W., & Fromm, M. (2009). Claudin-16 affects transcellular cl- secretion in mdck cells. *The Journal of Physiology*, *587*, 3777–3793. doi:10.1113/jphysiol.2009.173401.

Harel, I., Benayoun, B. A., Machado, B., Singh, P. P., Hu, C.-K., Pech, M. F., Valenzano, D. R., Zhang, E., Sharp, S. C., Artandi, S. E., & Brunet, A. (2015). A platform for rapid exploration of aging and diseases in a naturally short-lived vertebrate. *Cell*, *160*, 1013–1026. doi:10.1016/j.cell.2015.01.038.

He, J., Hsuchou, H., He, Y., Kastin, A. J., Wang, Y., & Pan, W. (2014). Sleep restriction impairs blood–brain barrier function. *Journal of Neuroscience*, *34*, 14697–14706. doi:10.1523/JNEUROSCI.2111-14.2014.

Ikenouchi, J., Furuse, M., Furuse, K., Sasaki, H., Tsukita, S., & Tsukita, S. (2005). Tricellulin constitutes a novel barrier at tricellular contacts of epithelial cells . *Journal of Cell Biology*, *171*, 939–945. doi:10.1083/jcb.200510043.

Ito, Y., Tanaka, H., Okamoto, H., & Ohshima, T. (2010). Characterization of neural stem cells and their progeny in the adult zebrafish optic tectum. *Developmental Biology*, *342*, 26–38. doi:10.1016/j.ydbio.2010.03.008.

Jin, S.-W., Beis, D., Mitchell, T., Chen, J.-N., & Stainier, D. Y. R. (2005). Cellular and molecular analyses of vascular tube and lumen formation in zebrafish. *Development*, *132*, 5199–5209. doi:10.1242/dev.02087.

Kim, Y., Nam, H. G., & Valenzano, D. R. (2016). The short-lived african turquoise killifish: an emerging experimental model for ageing. *Disease models & mechanisms*, *9*, 115–129. doi:10.1242/dmm.023226.

Kishi, S., Slack, B. E., Uchiyama, J., & Zhdanova, I. V. (2009). Zebrafish as a genetic model in biological and behavioral gerontology: Where development meets aging in vertebrates – a mini-review. *Gerontology*, *55*, 430–441. doi:10.1159/000228892.

Kiss, T., Nyúl-Tóth, Á., Balasubramanian, P., Tarantini, S., Ahire, C., DelFavero, J., Yabluchanskiy, A., Csipo, T., Farkas, E., Wiley, G., Garman, L., Csiszar, A., & Ungvari, Z. (2020). Single-cell rna sequencing identifies senescent cerebromicrovascular endothelial cells in the aged mouse brain. *GeroScience*, *42*, 429–444. doi:10.1007/s11357-020-00177-1.

Kluge, M. G., Abdolhoseini, M., Zalewska, K., Ong, L. K., Johnson, S. J., Nilsson, M., & Walker, F. R. (2019). Spatiotemporal analysis of impaired microglia process movement at sites of secondary neurodegeneration post-stroke. *Journal of Cerebral Blood Flow & Metabolism*, *39*, 2456–2470. doi:10.1177/0271678X18797346.

Konrad, M., Schaller, A., Seelow, D., Pandey, A. V., Waldegger, S., Lesslauer, A., Vitzthum, H., Suzuki, Y., Luk, J. M., Becker, C., Schlingmann, K. P., Schmid, M., Rodriguez-Soriano, J., Ariceta, G., Cano, F., Enriquez, R., Jüppner, H., Bakkaloglu, S. A., Hediger, M. A., Gallati, S., Neuhauss, S. C., Nürnberg, P., & Weber, S. (2006). Mutations in the tight-junction gene claudin 19 (cldn19) are associated with renal magnesium wasting, renal failure, and severe ocular involvement. *The American Journal of Human Genetics*, *79*, 949–957. doi:10.1086/508617.

Krause, G., Winkler, L., Mueller, S. L., Haseloff, R. F., Piontek, J., & Blasig, I. E. (2008). Structure and function of claudins. *Biochimica et Biophysica Acta (BBA) - Biomembranes*, *1778*, 631–645. doi:10.1016/j.bbamem.2007.10.018. Apical Junctional Complexes Part I.

Lee, H., & Pienaar, I. S. (2014). Disruption of the blood-brain barrier in parkinson's disease: curse or route to a cure? *Front Biosci (Landmark Ed)*, *19*, 272–80. doi:10.2741/4206.

Li, Y., Xie, L., Huang, T., Zhang, Y., Zhou, J., Qi, B., Wang, X., Chen, Z., & Li, P. (2019). Aging neurovascular unit and potential role of dna damage and repair in combating vascular and neurodegenerative disorders. *Frontiers in Neuroscience*, *13*, 778. doi:10.3389/fnins.2019.00778.

Lin, Y., Jiang, H., Liu, Y., Rosa Gameiro, G., Gregori, G., Dong, C., Rundek, T., & Wang, J. (2019). Age-related alterations in retinal tissue perfusion and volumetric vessel density. *Investigative Ophthalmology and Visual Science*, *60*, 685–693. doi:10.1167/iovs.18-25864.

López-Otín, C., Blasco, M. A., Partridge, L., Serrano, M., & Kroemer, G. (2013). The hallmarks of aging. *Cell*, *153*, 1194–1217. doi:10.1016/j.cell.2013.05.039.

Manuel, R., Gorissen, M., Stokkermans, M., Zethof, J., Ebbesson, L. O., Vis, H. v. d., Flik, G., & Bos, R. v. d. (2015). The effects of environmental enrichment and age-related differences on inhibitory avoidance in zebrafish (danio rerio hamilton). *Zebrafish*, *12*, 152–165. doi:10.1089/zeb.2014.1045.

Mattson, M. P., & Magnus, T. (2006). Ageing and neuronal vulnerability. *Nature Reviews Neuroscience*, *7*, 278–294. doi:10.1038/nrn1886.

Mineta, K., Yamamoto, Y., Yamazaki, Y., Tanaka, H., Tada, Y., Saito, K., Tamura, A., Igarashi, M., Endo, T., Takeuchi, K., & Tsukita, S. (2011). Predicted expansion of the claudin multigene family. *FEBS Letters*, *585*, 606–612. doi:10.1016/j.febslet.2011.01.028.

Montagne, A., Barnes, S. R., Sweeney, M. D., Halliday, M. R., Sagare, A. P., Zhao, Z., Toga, A. W., Jacobs, R. E., Liu, C. Y., Amezcua, L., Harrington, M. G., Chui, H. C.,

Law, M., & Zlokovic, B. V. (2015). Blood-brain barrier breakdown in the aging human hippocampus. *Neuron*, *85*, 296–302. doi:10.1016/j.neuron.2014.12.032.

Morita, K., Furuse, M., Fujimoto, K., & Tsukita, S. (1999). Claudin multigene family encoding four-transmembrane domain protein components of tight junction strands. *Proceedings of the National Academy of Sciences*, *96*, 511–516. doi:10.1073/pnas.96.2.511.

Münzel, E. J., Becker, C. G., Becker, T., & Williams, A. (2014). Zebrafish regenerate full thickness optic nerve myelin after demyelination, but this fails with increasing age. *Acta Neuropathologica Communications*, *2*, 77. doi:10.1186/s40478-014-0077-y.

Nation, D. A., Sweeney, M. D., Montagne, A., Sagare, A. P., D'Orazio, L. M., Pachicano, M., Sepehrband, F., Nelson, A. R., Buennagel, D. P., Harrington, M. G., Benzinger, T. L. S., Fagan, A. M., Ringman, J. M., Schneider, L. S., Morris, J. C., Chui, H. C., Law, M., Toga, A. W., & Zlokovic, B. V. (2019). Blood–brain barrier breakdown is an early biomarker of human cognitive dysfunction. *Nature Medicine*, *25*, 270–276. doi:10.1038/s41591-018-0297-y.

Nitta, T., Hata, M., Gotoh, S., Seo, Y., Sasaki, H., Hashimoto, N., Furuse, M., & Tsukita, S. (2003). Size-selective loosening of the blood-brain barrier in claudin-5-deficient mice . *Journal of Cell Biology*, *161*, 653–660. URL: 10.1083/jcb.200302070. doi:10.1083/jcb.200302070.

Ohtsuki, S., Sato, S., Yamaguchi, H., Kamoi, M., Asashima, T., & Terasaki, T. (2007). Exogenous expression of claudin-5 induces barrier properties in cultured rat brain capillary endothelial cells. *Journal of Cellular Physiology*, *210*, 81–86. doi:10.1002/jcp.20823.

Perry, V. H., & Holmes, C. (2014). Microglial priming in neurodegenerative disease. *Nature Reviews Neurology*, *10*, 217–224. doi:10.1038/nrneurol.2014.38.

Peters, A. (2009). The effects of normal aging on myelinated nerve fibers in monkey central nervous system. *Frontiers in neuroanatomy*, *3*, 11. doi:10.3389/neuro.05.011.2009.

Pöyhönen, S., Er, S., Domanskyi, A., & Airavaara, M. (2019). Effects of neurotrophic factors in glial cells in the central nervous system: Expression and properties in neurodegeneration and injury. *Frontiers in Physiology*, *10*, 486. doi:10.3389/fphys.2019.00486.

Resnick, M. B., Gavilanez, M., Newton, E., Konkin, T., Bhattacharya, B., Britt, D. E., Sabo, E., & Moss, S. F. (2005). Claudin expression in gastric adenocarcinomas: a tissue microarray study with prognostic correlation. *Human Pathology*, *36*, 886–892. doi:10.1016/j.humpath.2005.05.019.

Schrag, A., Horsfall, L., Walters, K., Noyce, A., & Petersen, I. (2015). Prediagnostic presentations of parkinson's disease in primary care: a case-control study. *The Lancet Neurology*, *14*, 57–64. doi:10.1016/S1474-4422(14)70287-X.

Segarra, M., Aburto, M. R., & Acker-Palmer, A. (2021). Blood–brain barrier dynamics to maintain brain homeostasis. *Trends in Neurosciences*, (pp. 393–405). doi:10.1016/j.tins.2020.12.002.

Shatzmiller, S., Lapidot, I., & Zats, G. M. (2019). Blood brain barrier crossing for therapeutic and diagnostic agents.

Shimoda, N., Izawa, T., Yoshizawa, A., Yokoi, H., Kikuchi, Y., & Hashimoto, N. (2014). Decrease in cytosine methylation at cpg island shores and increase in dna fragmentation during zebrafish aging. *AGE*, *36*, 103–115. doi:10.1007/s11357-013-9548-5.

Skaper, S. D., Facci, L., Zusso, M., & Giusti, P. (2017). Synaptic plasticity, dementia and alzheimer disease. *CNS & Neurological Disorders - Drug Targets*, *16*, 220–233. doi:10.2174/1871527316666170113120853.

Stamatovic, S. M., Martinez-Revollar, G., Hu, A., Choi, J., Keep, R. F., & Andjelkovic, A. V. (2019). Decline in sirtuin-1 expression and activity plays a critical role in blood-brain barrier permeability in aging. *Neurobiology of Disease*, *126*, 105–116. doi:10.1016/j.nbd.2018.09.006.

Steverson, M. (2018). Ageing and health. URL: https://www.who.int/news-room/fact-sheets/detail/ageing-and-health.

Streit, W. J., Sammons, N. W., Kuhns, A. J., & Sparks, D. L. (2004). Dystrophic microglia in the aging human brain. *Glia*, *45*, 208–212. doi:10.1002/glia.10319.

Tebbe, B., Mankertz, J., Schwarz, C., Amasheh, S., Fromm, M., Assaf, C., Schultz-Ehrenburg, U., Sánchez Ruderisch, H., Schulzke, J.-D., & Orfanos, C. (2002). Tight junction proteins: a novel class of integral membrane proteins. *Archives of Dermatological Research*, *294*, 14–18. doi:10.1007/s00403-001-0290-y.

Traver, D., Herbomel, P., Patton, E. E., Murphey, R. D., Yoder, J. A., Litman, G. W., Catic, A., Amemiya, C. T., Zon, L. I., & Trede, N. S. (2003). The zebrafish as a model organism to study development of the immune system. *Adv Immunol*, *81*, 253–330.

Van houcke, J., De Groef, L., Dekeyster, E., & Moons, L. (2015). The zebrafish as a gerontology model in nervous system aging, disease, and repair. *Ageing Research Reviews*, *24*, 358–368. doi:10.1016/j.arr.2015.10.004.

Weller, J., & Budson, A. (2018). Current understanding of alzheimer's disease diagnosis and treatment. *F1000Research*, *7*, F1000 Faculty Rev–1161.

Wilcox, E. R., Burton, Q. L., Naz, S., Riazuddin, S., Smith, T. N., Ploplis, B., Belyantseva, I., Ben-Yosef, T., Liburd, N. A., Morell, R. J., Kachar, B., Wu, D. K., Griffith, A. J., Riazuddin, S., & Friedman, T. B. (2001). Mutations in the gene encoding tight junction claudin-14 cause autosomal recessive deafness dfnb29. *Cell*, *104*, 165–172. doi:10.1016/S0092-8674(01)00200-8.

Wolburg, H., Wolburg-Buchholz, K., Kraus, J., Rascher-Eggstein, G., Liebner, S., Hamm, S., Duffner, F., Grote, E.-H., Risau, W., & Engelhardt, B. (2003). Localization of claudin-3 in tight junctions of the blood-brain barrier is selectively lost during experimental autoimmune encephalomyelitis and human glioblastoma multiforme. *Acta Neuropathologica*, *105*, 586–592. doi:10.1007/s00401-003-0688-z.

Zeppenfeld, D. M., Simon, M., Haswell, J. D., D'Abreo, D., Murchison, C., Quinn, J. F., Grafe, M. R., Woltjer, R. L., Kaye, J., & Iliff, J. J. (2017). Association of Perivascular Localization of Aquaporin-4 With Cognition and Alzheimer Disease in Aging Brains . *JAMA Neurology*, *74*, 91–99. doi:10.1001/jamaneurol.2016.4370.